TMDs from lattice QCD

Michael Wagman

QCD@LHC 2024

October 10, 2024

Cross sections and TMDs

High-energy cross sections factorize: *(perturbative coefficient) x (structure function)*

Deep inelastic scattering (DIS): $\sigma(Q^2) \sim \int dx\ H(Q^2, x, \mu)\ f_{q/A}(x, \mu)$

$$\ell + A \to \ell' + X$$

PDF ~ probability of parton q carrying momentum fraction x of hadron (or nucleus) A

Semi-inclusive DIS (SIDIS): $\sigma(Q^2, q_T) \sim \int dx\ H(Q^2, q_T, x, \mu)\ f_{q/A}^{\rm TMD}(q_T, x, \mu) D_{h/q}(q_T, x)$

$$\ell + A \to \ell' + h + X$$

Transverse Momentum Dependent PDF

Fragmentation function

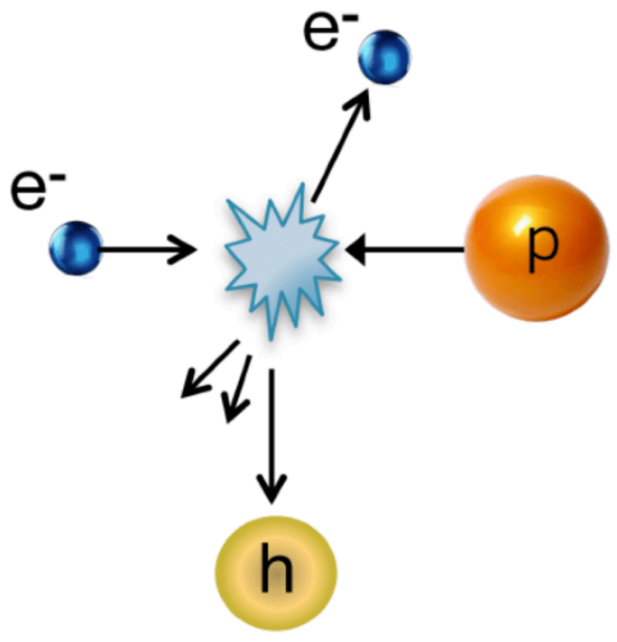

TMDPDFs needed to predict Drell-Yan, SIDIS, …

The *W* boson mass

Precise measurement of M_W from CDF disagrees at 7 sigma with M_W obtained from electroweak precision fits

New physics?

Robust understanding of all QCD theory uncertainties essential

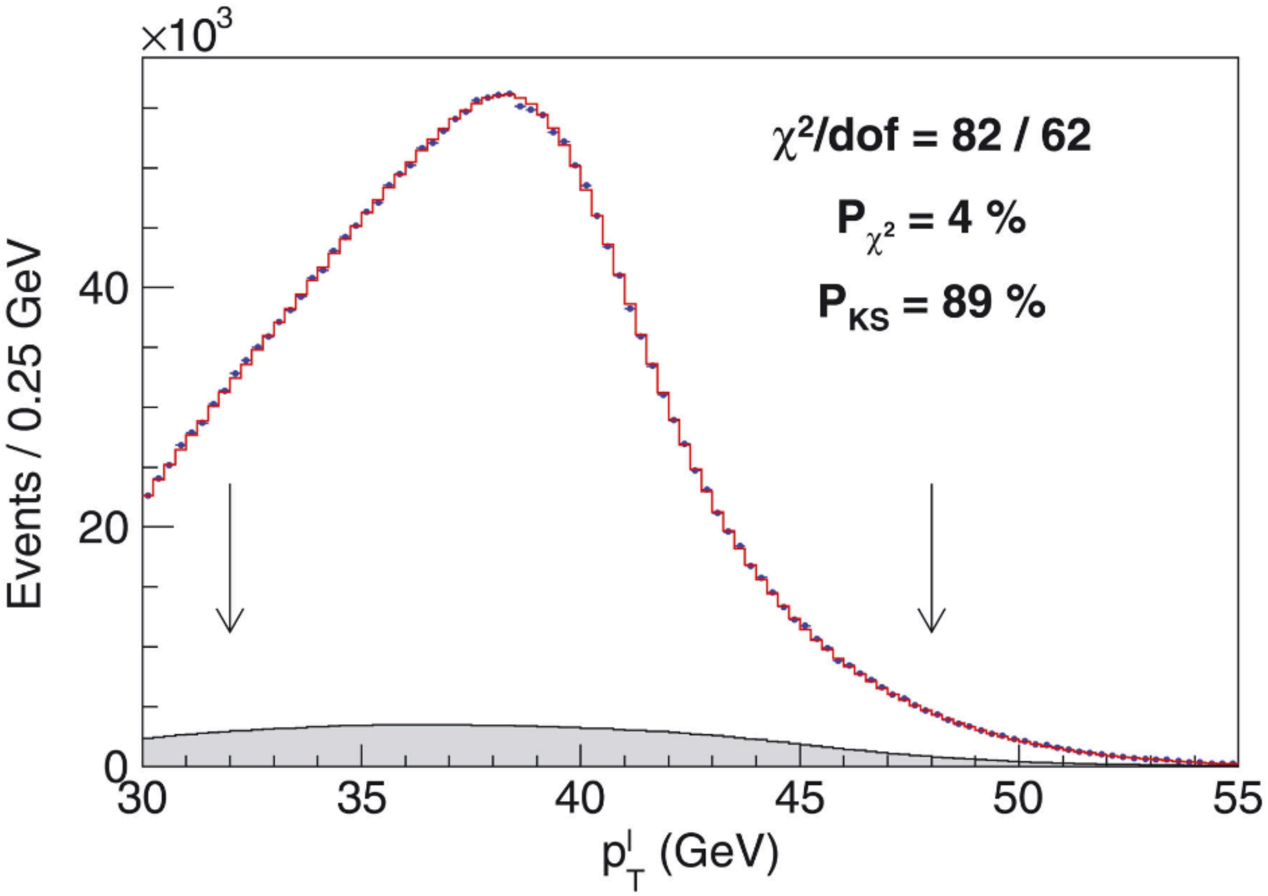

Aaltonen et al [CDF], Science 376 (2022)

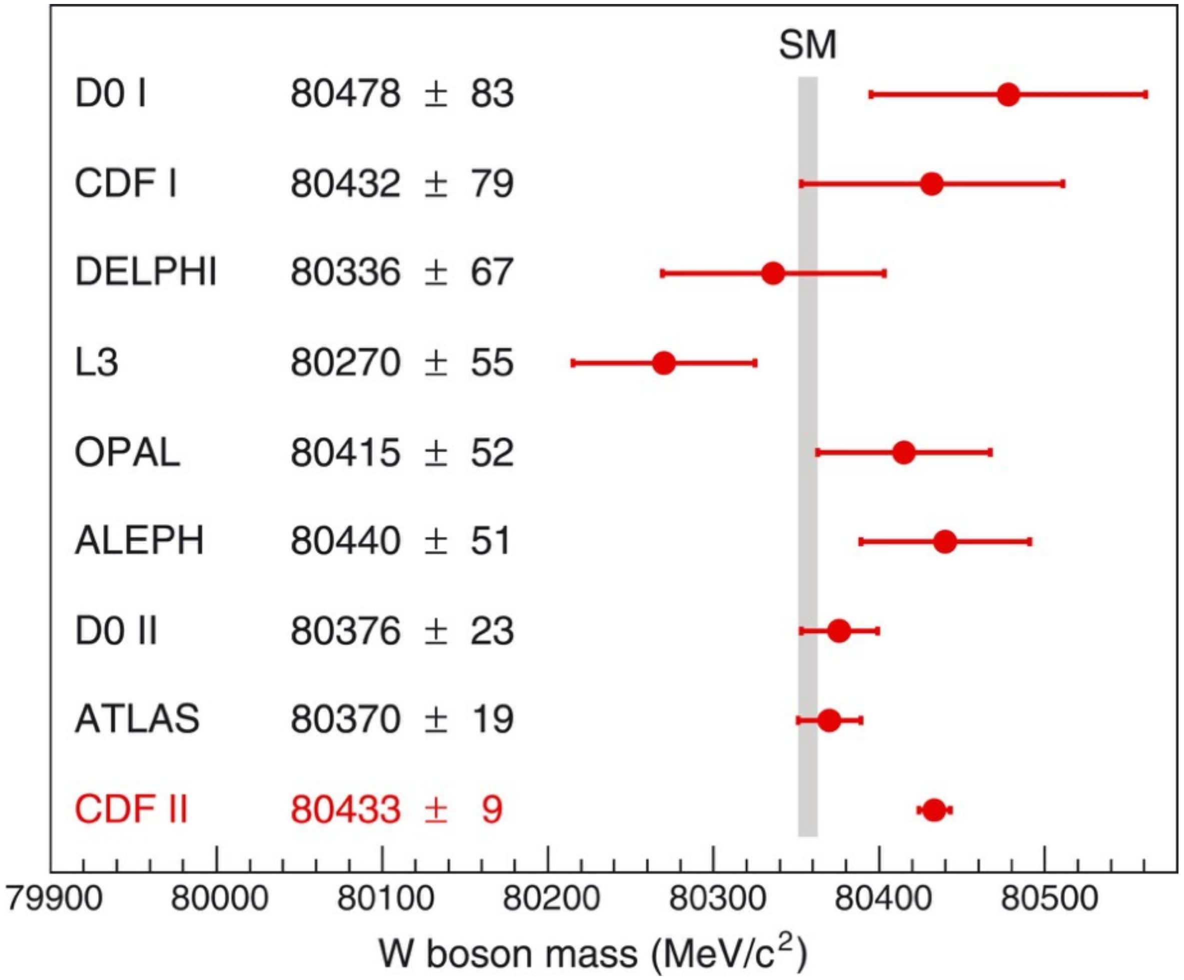

Measurement made by fitting shapes of transverse momentum distributions to theory predictions including resumed and nonperturbative QCD effects

Distribution shapes are insensitive to many aspects of TMDPDFs but sensitive to flavor dependence and **"rapidity evolution"**

The Collins-Soper kernel

TMDPDFs depend on UV renormalization scale μ as well as a scale $\zeta \sim Q^2$ associated with the renormalization of rapidity divergences

$$f_{q/A}^{\mathrm{TMD}}(x, \vec{b}_T, \mu, \zeta) = f_{q/A}^{\mathrm{TMD}}(x, \vec{b}_T, \mu_0, \zeta_0)$$

$$\times \exp\left[\int_{\mu_0}^{\mu} \frac{d\mu'}{\mu'} \gamma_\mu^q(\mu', \zeta_0)\right] \exp\left[\frac{1}{2}\gamma_\zeta^q(\mu, b_T) \ln \frac{\zeta}{\zeta_0}\right]$$

UV anomalous dimension

Collins-Soper kernel

(rapidity anomalous dimension)

- Changing hard momentum scales requires evolving TMDPDFs in μ and ζ
- Evolution in μ is perturbative as long as μ is large, but evolution in ζ is always nonperturbative for $b_T \gtrsim \Lambda_{\mathrm{QCD}}^{-1}$
- Both anomalous dimensions are **independent of the hadron target**

CS kernel phenomenology

Fits to SIDIS and Drell-Yan data with multiple energy scales are sensitive to evolution effects and therefore the CS kernel

CS kernel can be extracted along with TMDPDF in global fits

SV19 - Scimemi and Vladimirov, JEHP 06 (2020)

(582 SIDIS + 457 DY data points)

Pavia19 - Bacchetta et al, JEHP 07 (2020)

(353 DY data points)

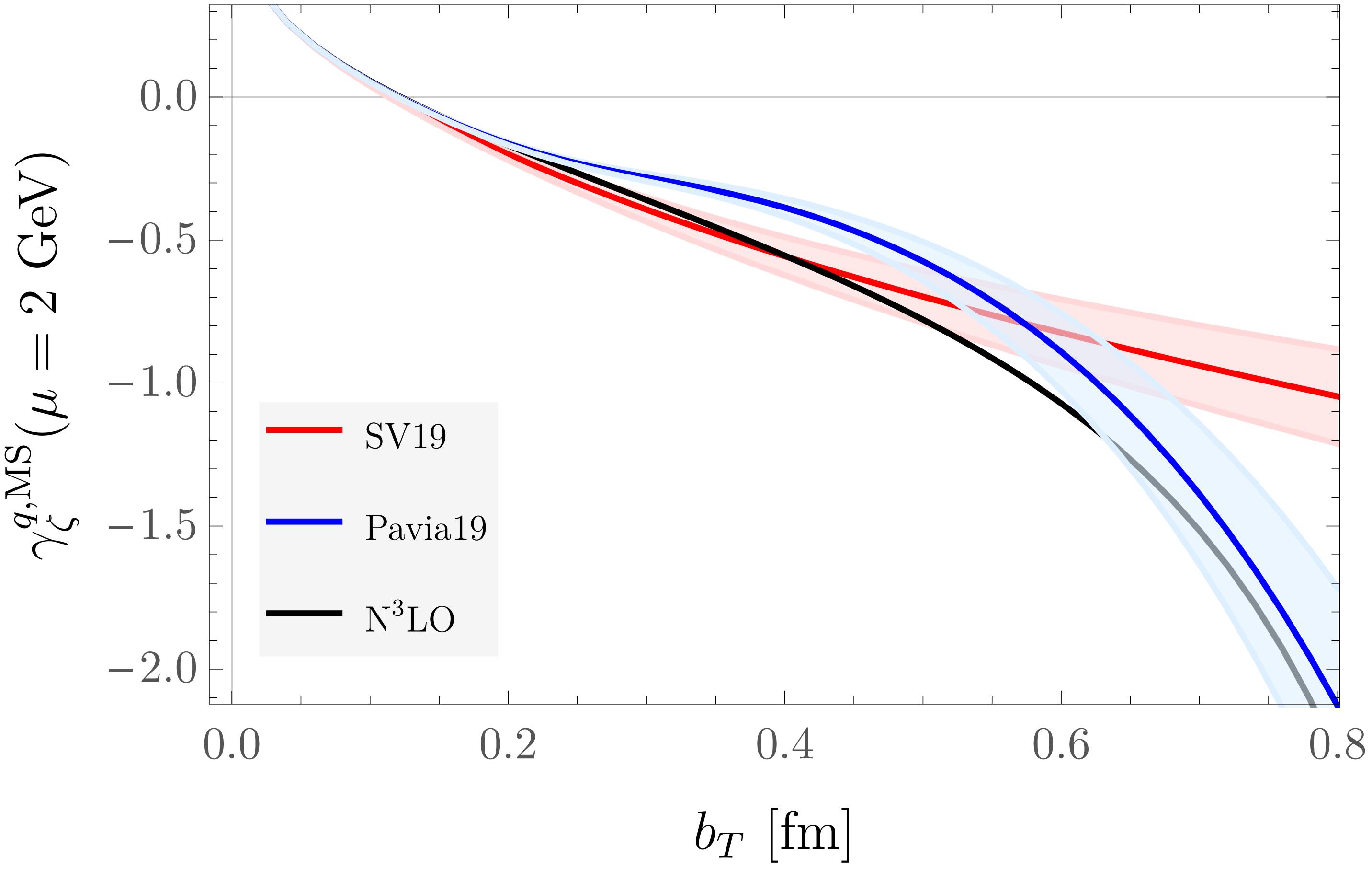

Modeling significant for

$$b_T \gtrsim 0.2\ \mathrm{fm}$$

(nonperturbative region)

Can we constrain the large b_T behavior of the CS kernel using lattice QCD?

Quasi TMDPDFs

The construction of quasi TMDPDFs is more complicated than collinear PDFs

Ji, PRL 110 (2013)

TMDPDF products appearing in e.g. Drell-Yan can be expressed as convolutions of "beam functions" and "soft functions"

Quasi beam functions can be constructed that are related to light-cone beam functions by a Lorentz boost

$$\widetilde{q}(x, b_T, P_z) = \lim_{\eta \to \infty} \int_{-\infty}^{\infty} \frac{dz}{4\pi} \, e^{-ixzP_z} \left\langle h(P_z) | \overline{q}(b_T) \gamma_4 W(b_T, \eta + b_T) W_T^\dagger(\eta + b_T, \eta) W_z^\dagger(\eta, 0) q(0) | h(P_Z) \right\rangle$$

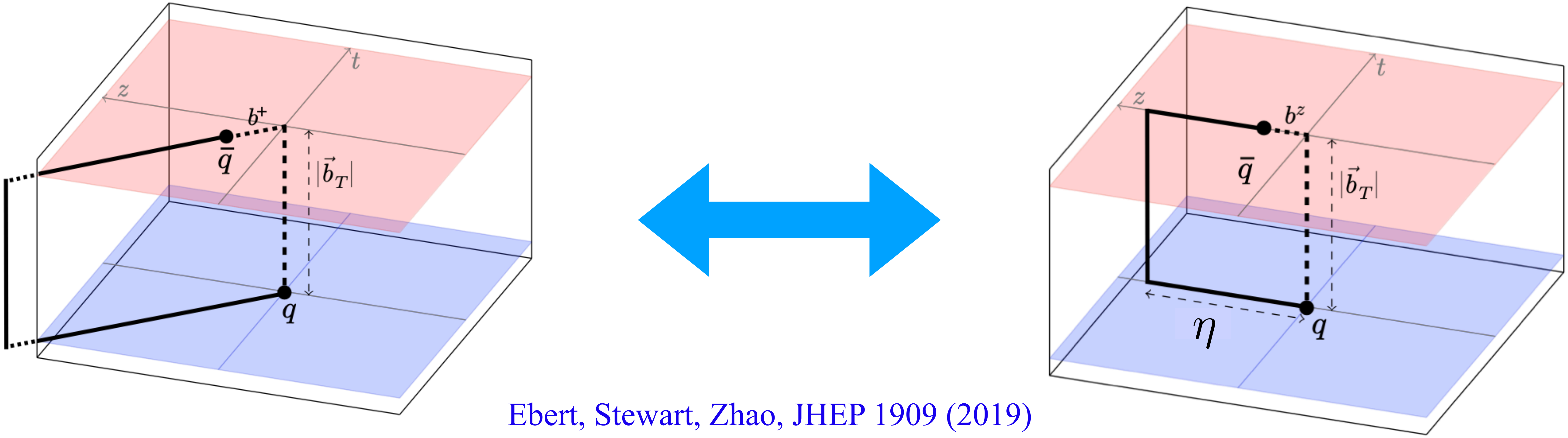

Ebert, Stewart, Zhao, JHEP 1909 (2019)

The soft function

TMDPDF products in Drell-Yan also involve a soft function that depends on the light-like momenta of both hadrons

Soft function cannot be related to a matrix element of equal-time operator product by a Lorentz boost

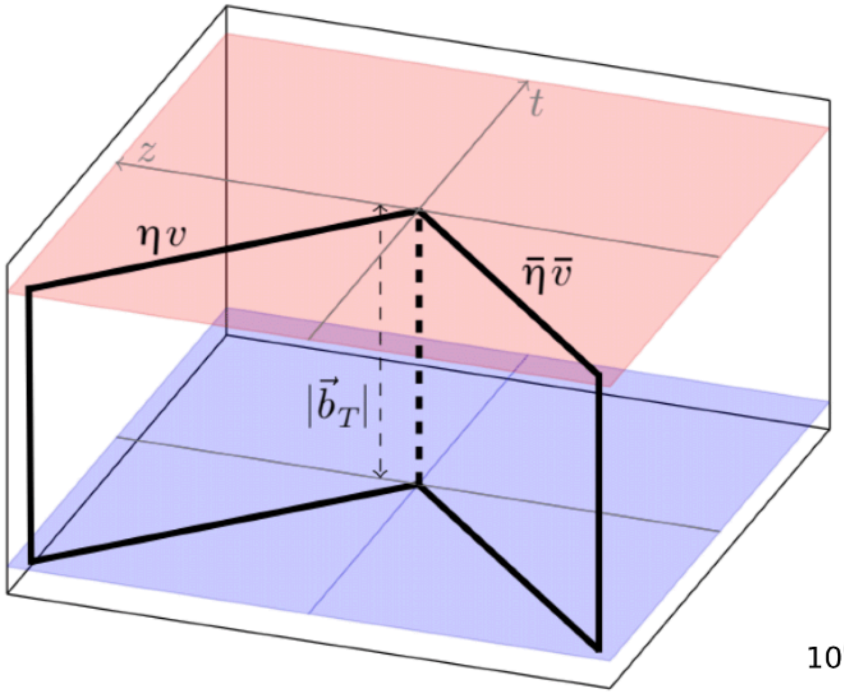

Recent progress relates light-cone soft function to a large-momentum form factor that can be calculated with LQCD

Ji, Liu, and Liu, Nucl Phys B 955 (2020)

Proof of principle demonstration that LQCD can predict TMDPDFs

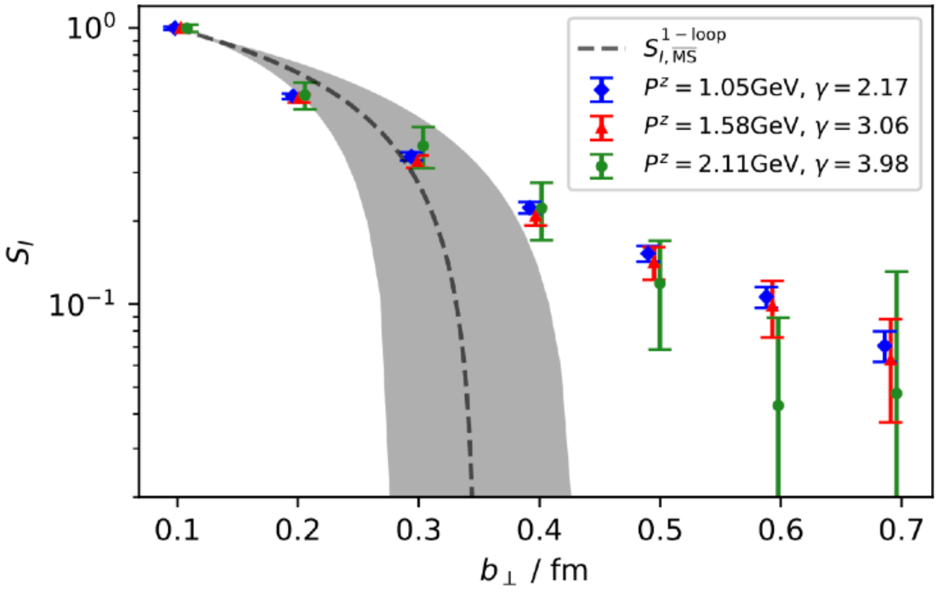

Zhang et al [LPC], PRL 125 (2020)

The CS kernel from LQCD

Ratios of TMDPDFs free from soft factors and can be calculated with LQCD

Musch et al, PRD 85 (2012)   Engelhardt et al, PRD 93 (2016)   Yoon et al, PRD 96 (2017)

CS kernel determination using quasi-TMDPDFs suggested:

Ji, Sun, Xiong, Yuan PRD 91 (2015)

Method concretely relating CS kernel to quasi TMDPDF ratios proposed and derived:

Ebert, Stewart, Zhao, PRD 99 (2019)

Euclidean quasi-beam function

$$\gamma_\zeta^{q,\overline{\mathrm{MS}}}(b_T,\mu) = 2\zeta \frac{d}{d\zeta} \ln f_{q/A}^{\mathrm{TMD},\overline{\mathrm{MS}}}(x, b_T, \mu, \zeta)$$

$$= \frac{1}{\ln(P_1^z/P_2^z)} \ln \frac{C_{\mathrm{TMD}}^{\overline{\mathrm{MS}}}(\mu, xP_2^z) \int db^z e^{ib^z x P_1^z}\, \widetilde{B}_{q/A}^{\overline{\mathrm{MS}}}(b^z, b_T, \eta, \mu, P_1^z)}{C_{\mathrm{TMD}}^{\overline{\mathrm{MS}}}(\mu, xP_1^z) \int db^z e^{ib^z x P_2^z}\, \widetilde{B}_{q/A}^{\overline{\mathrm{MS}}}(b^z, b_T, \eta, \mu, P_2^z)}$$

Perturbative matching factor known at NNLO

First LQCD exploration

CS kernel is a property of QCD vacuum, independent of hadronic state

We can learn about nuclear interactions using pion states!

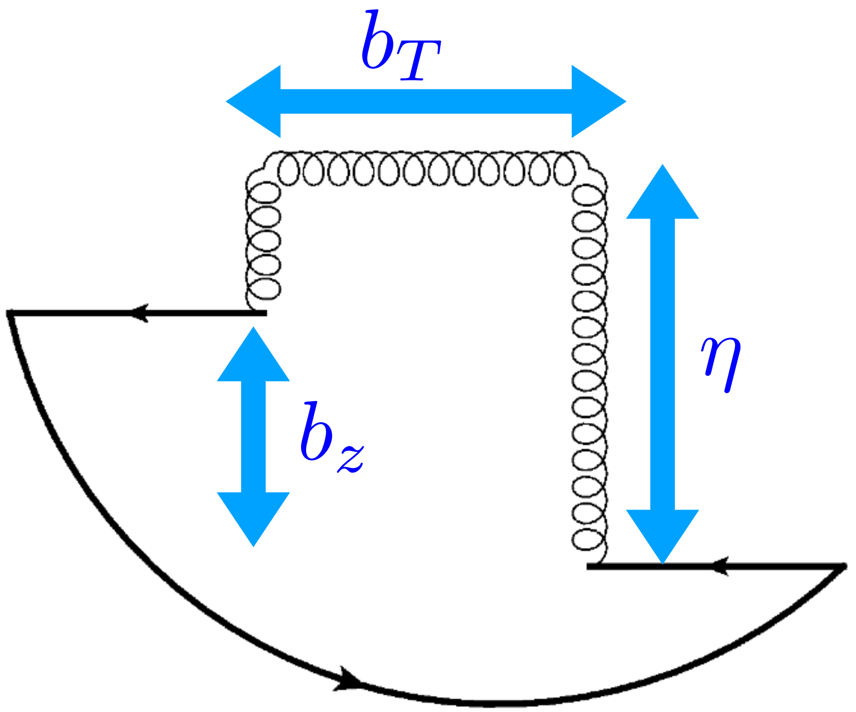

In quenched ($N_f = 0$) QCD, exact results calculable using heavy quark probe

$$m_\pi \sim 1.2 \text{ GeV}$$

Allows high precision with only 400 quark propagator sources

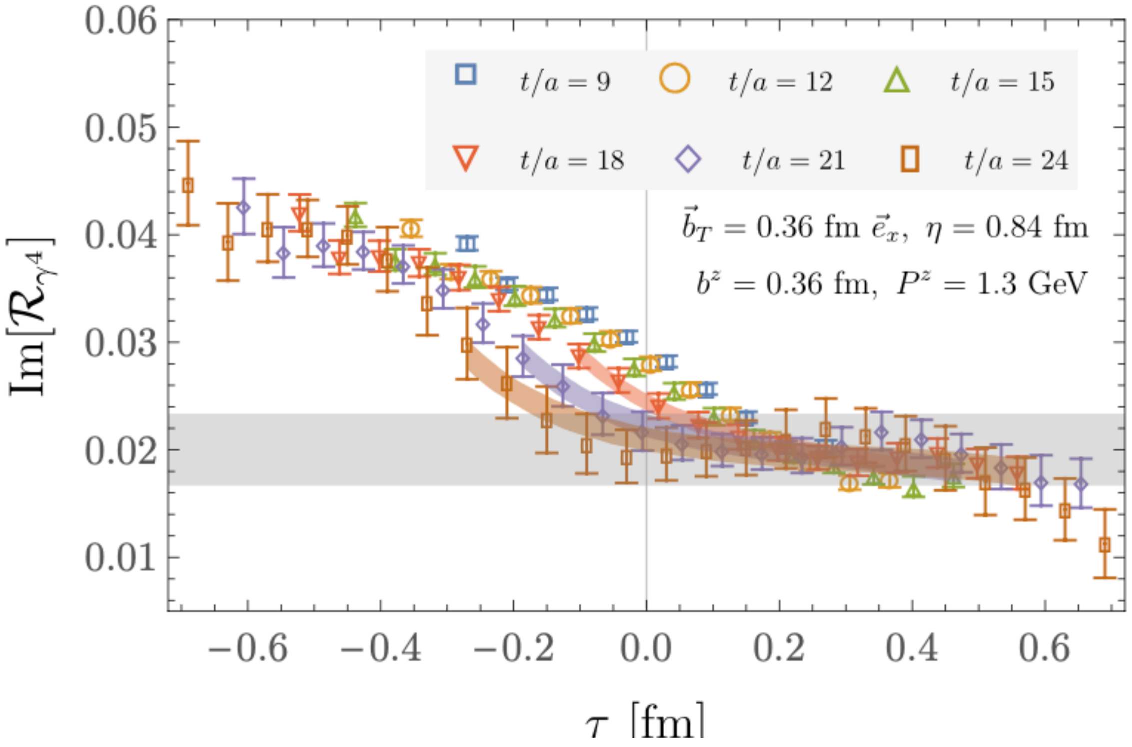

Shanahan, MW, Zhao, PRD 102 (2020)

3 values of $\eta \in [0.6, \ 0.8]$ fm

3 values of $P^z \in [1.3, \ 2.6]$ GeV

All 16 Dirac structures and staple geometries b_T and b^z

35,660 bare matrix elements - robust automated fitting essential

Quenched LQCD results

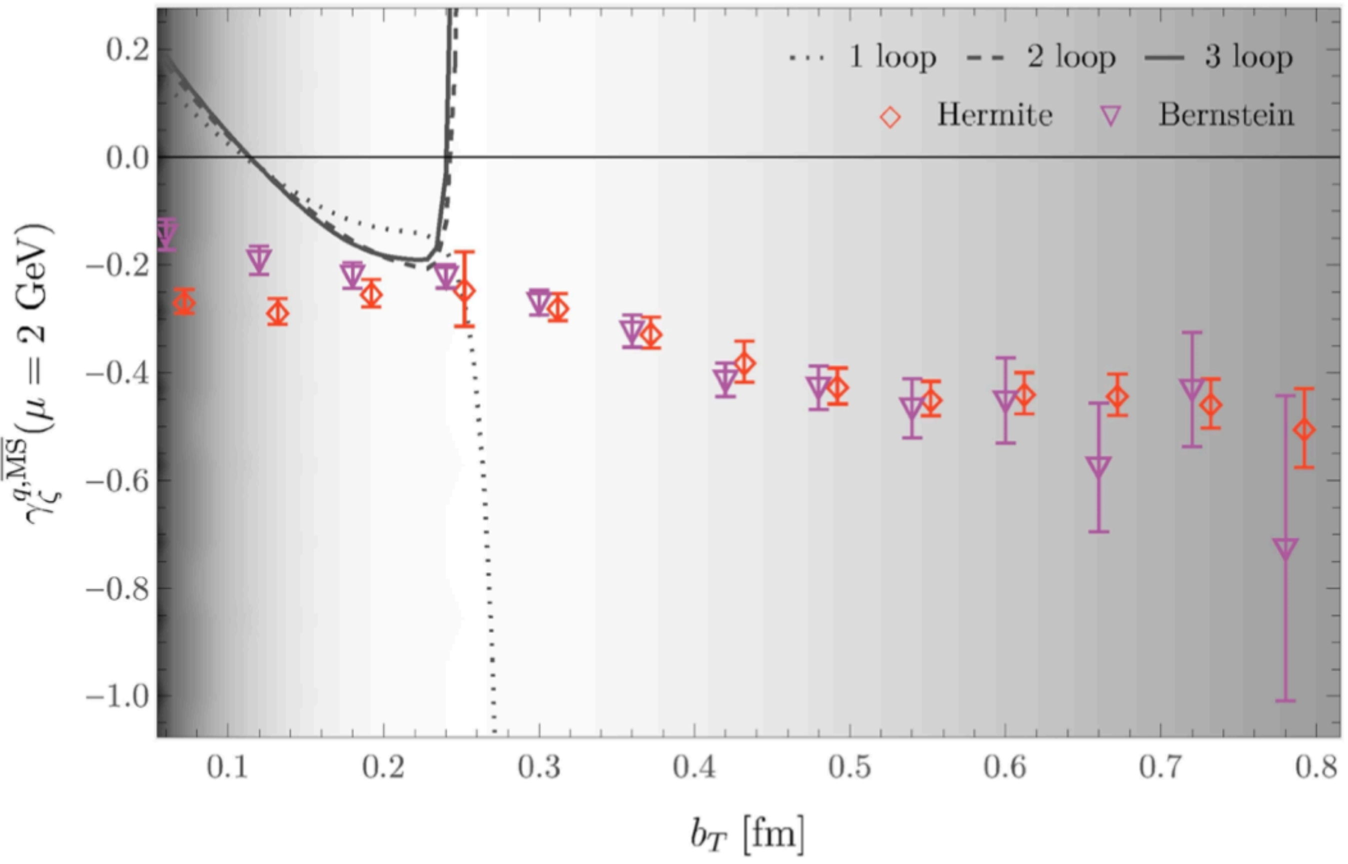

Shanahan, MW, Zhao, PRD 102 (2020)

CS kernel determined precisely for b_T extending into nonperturbative regime

Fourier transform truncation effects challenging to quantify, two different models used to extrapolate beam functions outside range of data

Shading denotes relative size of hard-to-quantify systematics

$m_\pi = 1.2$ GeV

$L = 32a = 1.92$ fm

$P^z \in \{1.3,\ 1.9,\ 2.6\}$ GeV

$\eta \leq 0.8$ fm

Fourier transform challenges

Fourier transform truncation effects: challenging systematic uncertainties to quantify

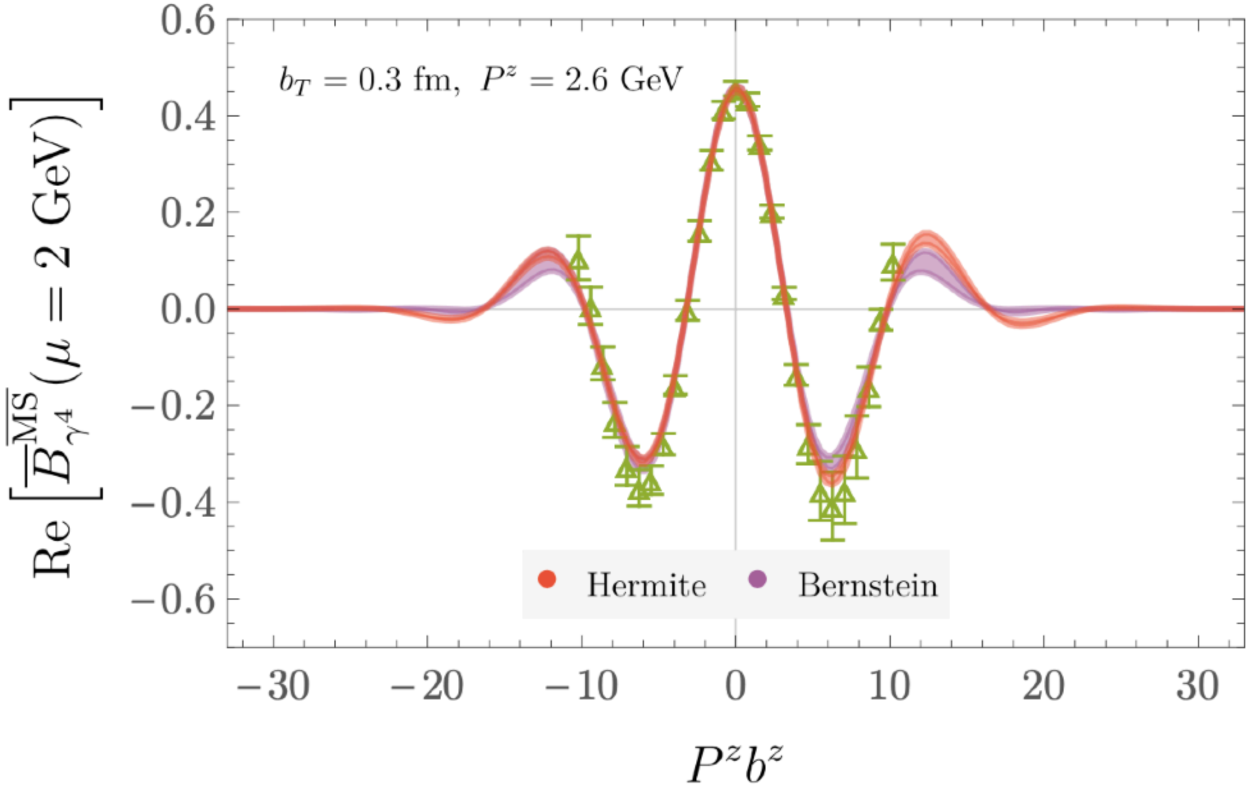

Shanahan, MW, Zhao, PRD 102 (2020)

Modeling of beam functions outside region with LQCD results necessary to cover region where Fourier transform integrand matters

Broadening of the (physical) beam function with increasing b_T leads to larger truncation effects

Unexpected asymmetry visible at large b_T

Renormalization issues?

Finite volume effects?

Briceño, Guerrero, Hansen, and Monahan, PRD 99 (2018)

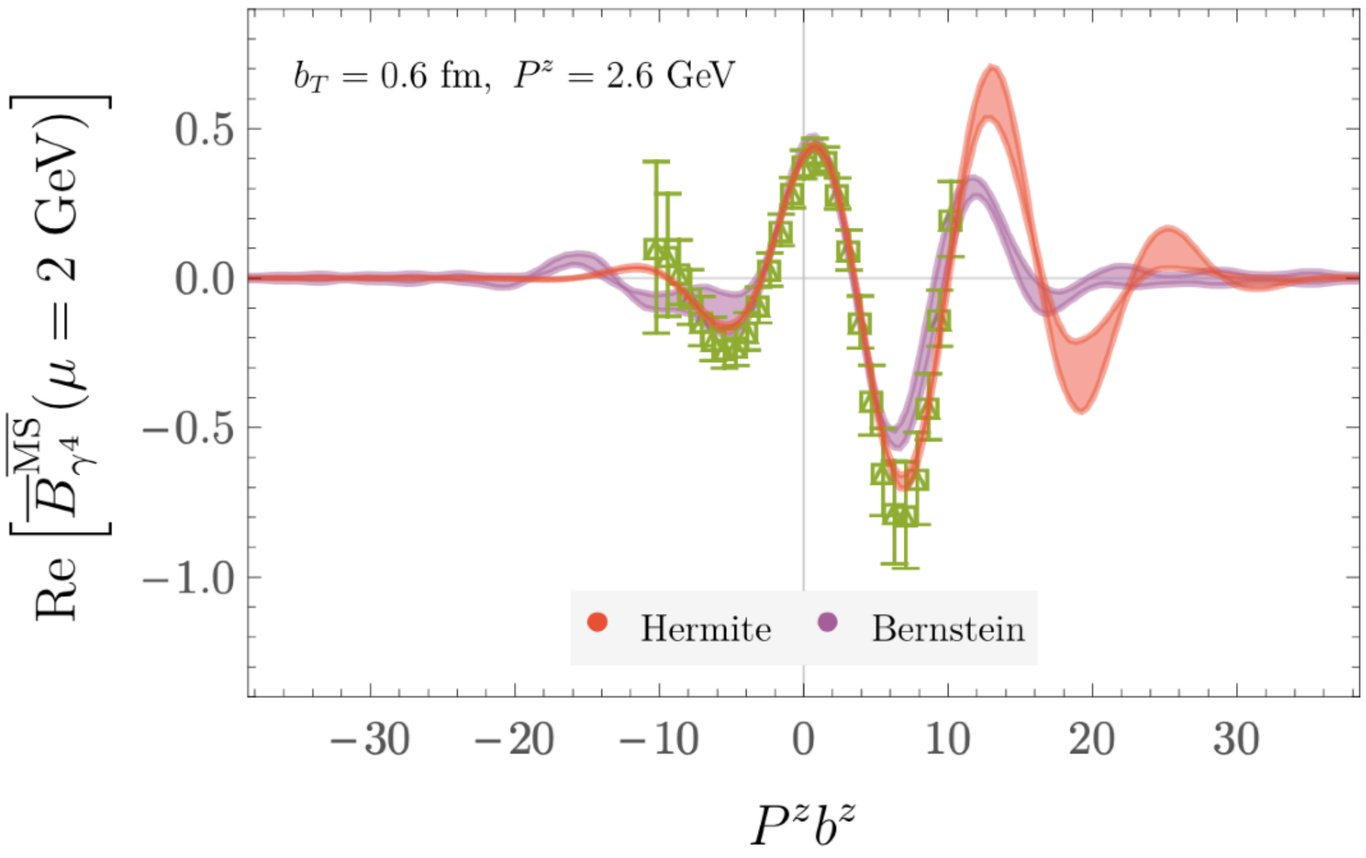

Dynamical LQCD exploration

Mixed action: $N_f = 2+1+1$ MILC ensembles with ~physical quark masses

$a = 0.12$ fm $\quad L = 48a = 5.6$ fm $\quad$ Bazavov et al [MILC] PRD 87 (2013)

- Wilson valence quarks with tree-level clover improvement, $m_\pi = 538(1)\ \mathrm{MeV}$

- Wilson flow (fixed in lattice units) used as smearing in valence action to reduce statistical noise

- Larger physical volume enable larger staple extents than in quenched calculation $\eta \leq 1.7$ fm

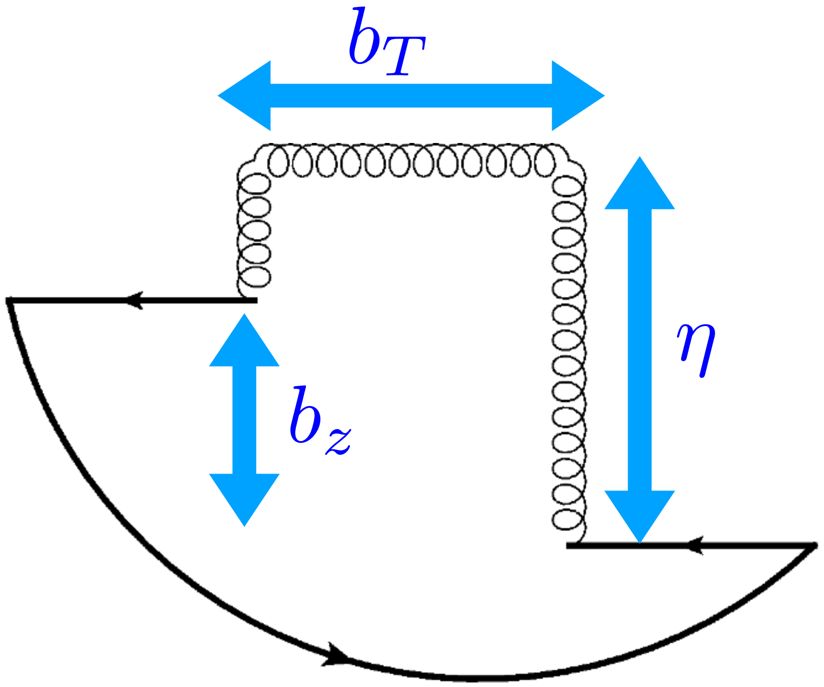

$(b^z P^z)_{\max} = 14.5$ vs quenched $(b^z P^z)_{\max} = 11$

Shanahan, MW, Zhao, PRD 104 (2021)

Renormalization and mixing

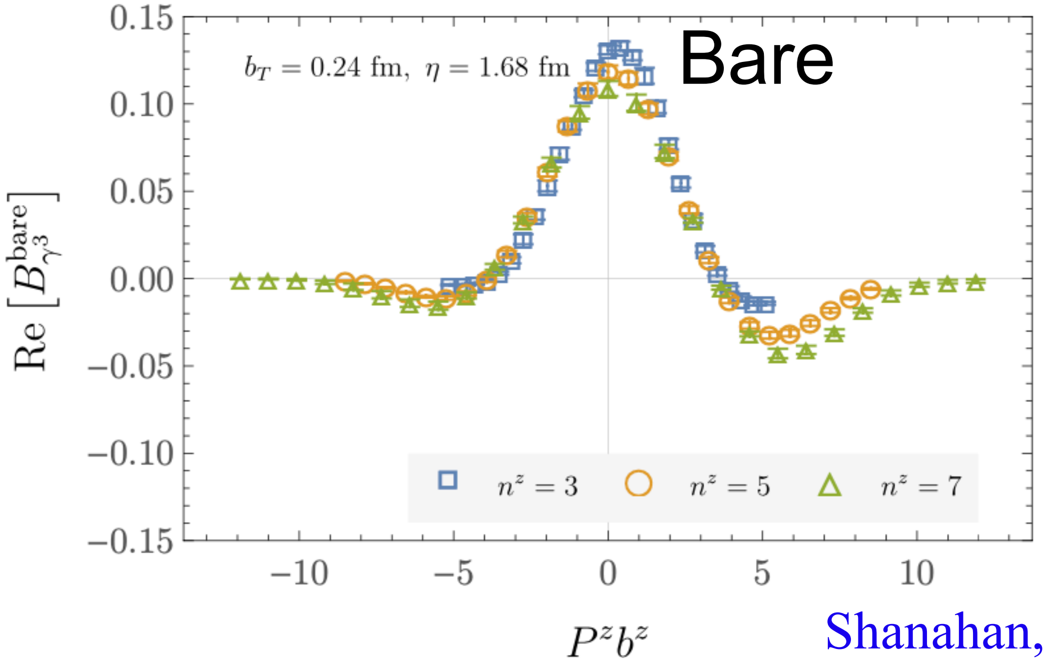

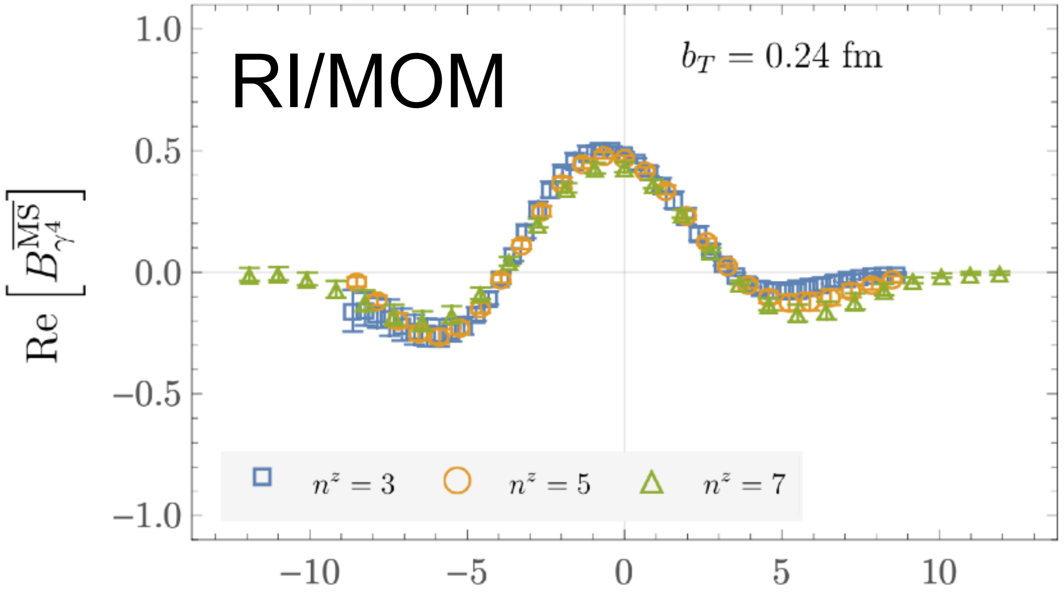

Shanahan, MW, Zhao, PRD 104 (2021)

Asymmetry persists in large volume using standard RI/MOM renormalization

Related issues seen in other calculations applying RI/MOM to nonlocal operators

Zhang et al [χQCD], PRD 104 (2021)

Huo et al [LPC], Nucl. Phys. B 969 (2021)

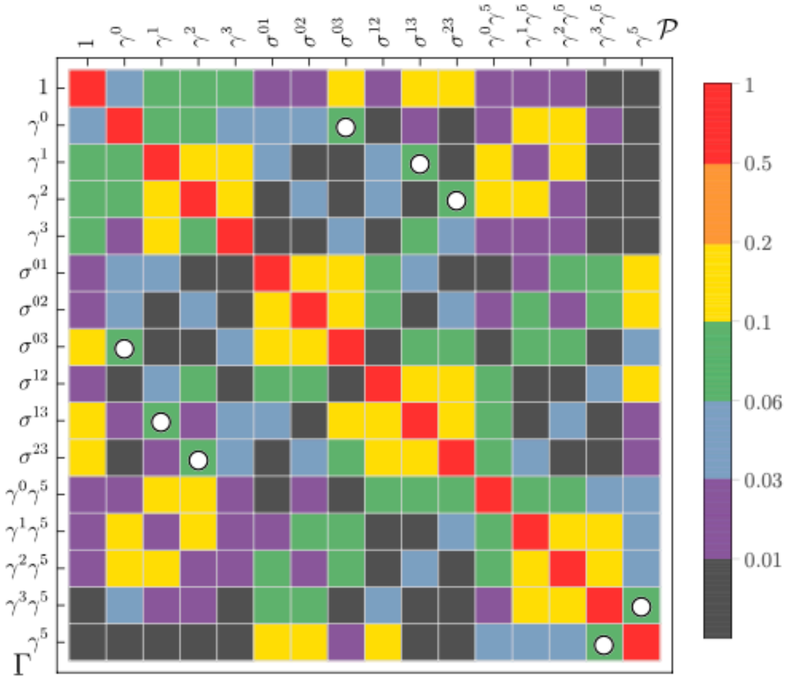

Shanahan, MW, Zhao, PRD 101 (2020)

Operator mixing predicted by 1-loop lattice perturbation theory (white dots) does not capture large nonperturbative effects

Constantinou, Panagopoulos, Spanoudes,
PRD 99 (2019)

Implies large UV-finite effects in RI/MOM scheme

CS kernel systematics

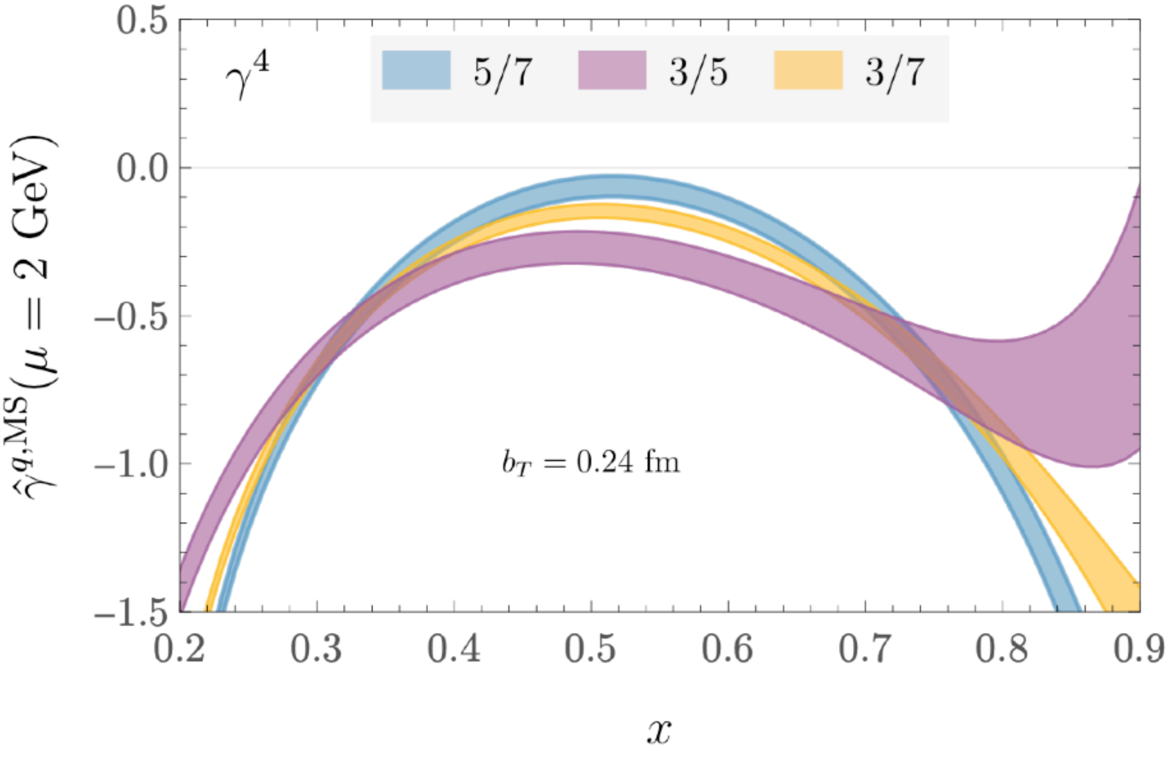

Still significant Fourier transform systematics

- x-dependence of CS kernel not successfully cancelled
- Differences between estimates with different momentum pairs visible

NLO quasi/light-cone matching effects significant

- Approximations valid only at LO used in previous calculations insufficient

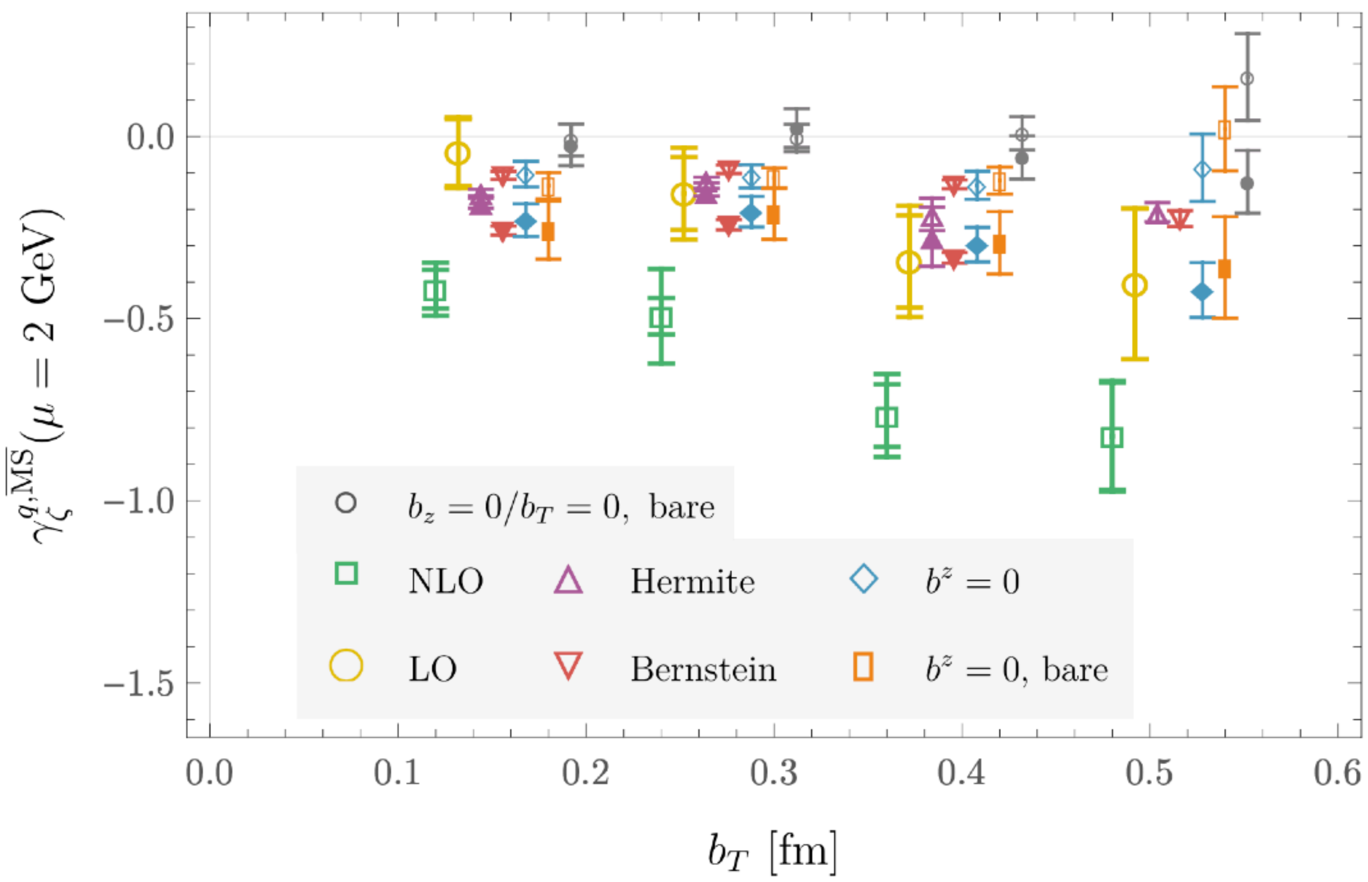

Shanahan, MW, Zhao, PRD 104 (2021)

CS kernel systematics

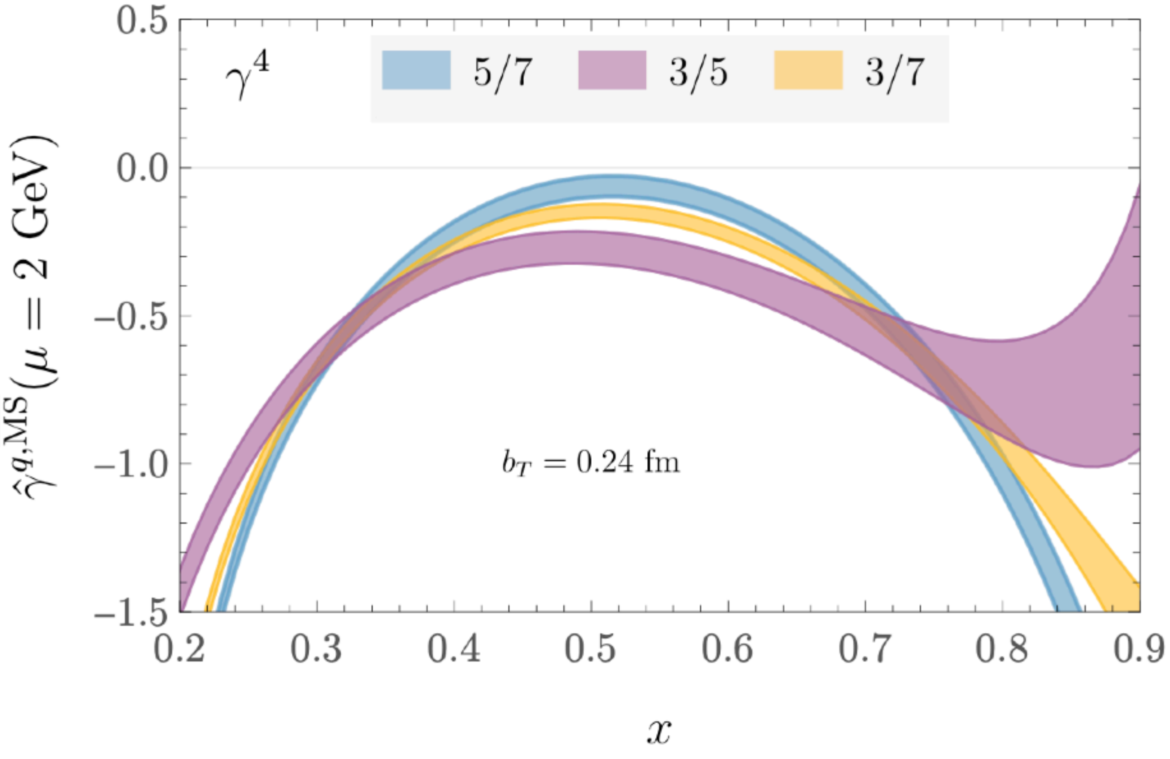

Still significant Fourier transform systematics

- x-dependence of CS kernel not successfully cancelled
- Differences between estimates with different momentum pairs visible

NLO quasi/light-cone matching effects significant

- Approximations valid only at LO used in previous calculations insufficient

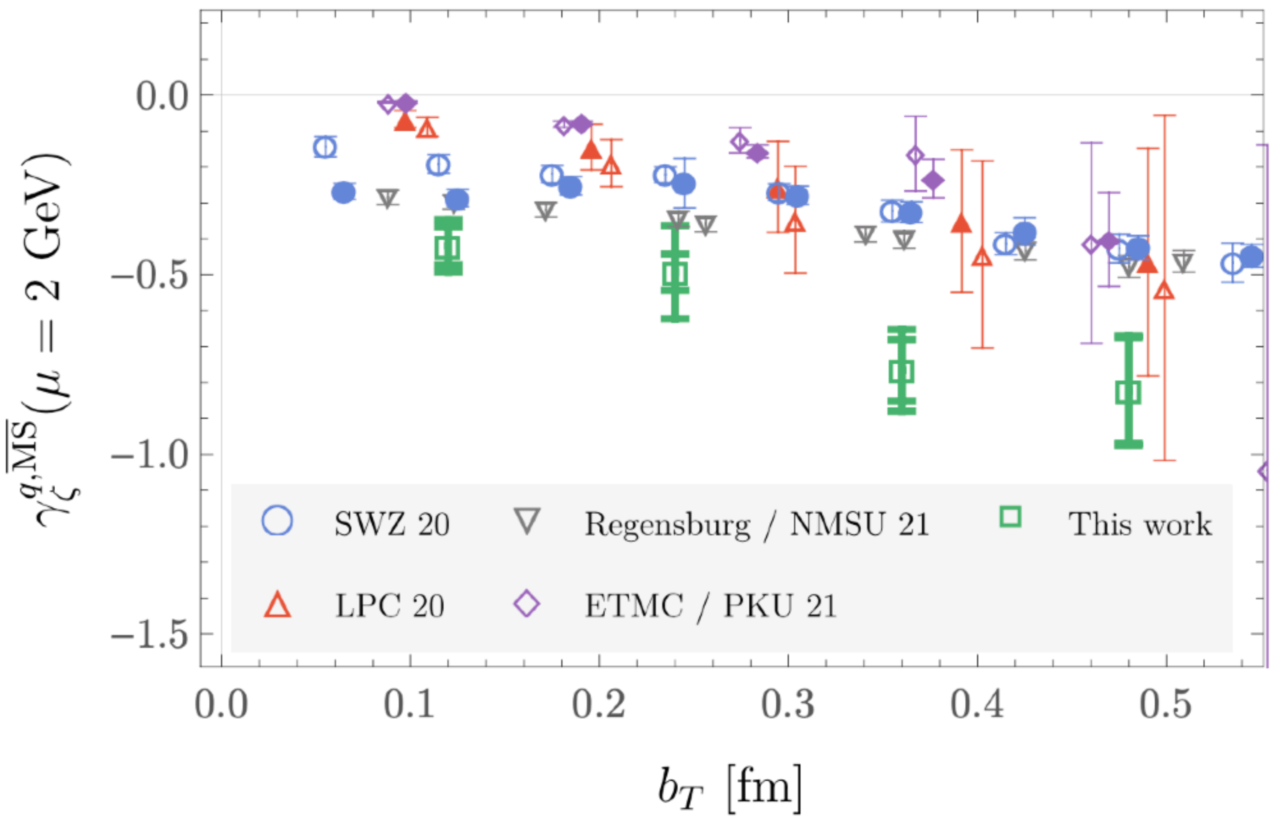

Shanahan, MW, Zhao, PRD 104 (2021)

TMD wavefunctions

The CS kernel can also be extracted from ratios of TMD wavefunctions analogous to distribution amplitudes

$$\tilde{\psi}(b^z, b_T, \eta, P^z) \propto \langle 0 | \mathcal{O}(b^z, b_T, \eta) | \pi(P^z) \rangle$$

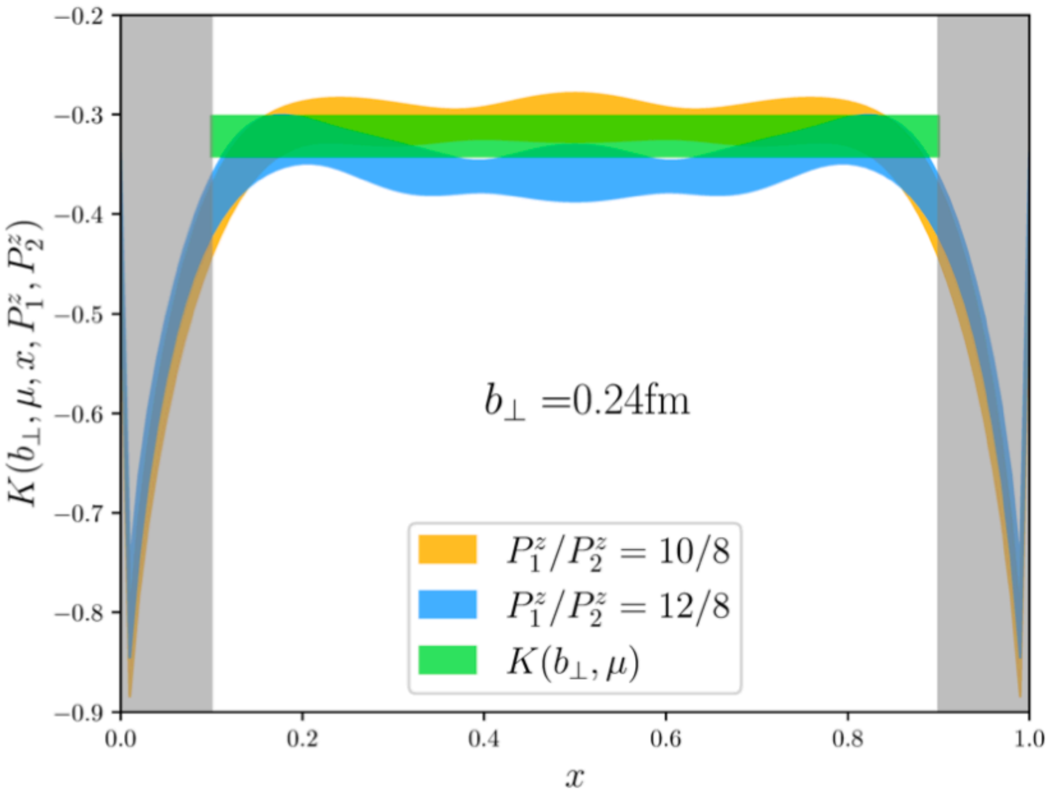

LPC collaboration found TMD wavefunctions with more symmetric staple geometries enable higher precision, improved Fourier transform systematics

Chu et al [LPC], PRD 106 (2022)

Results broadly consistent with previous LQCD calculations and phenomenology

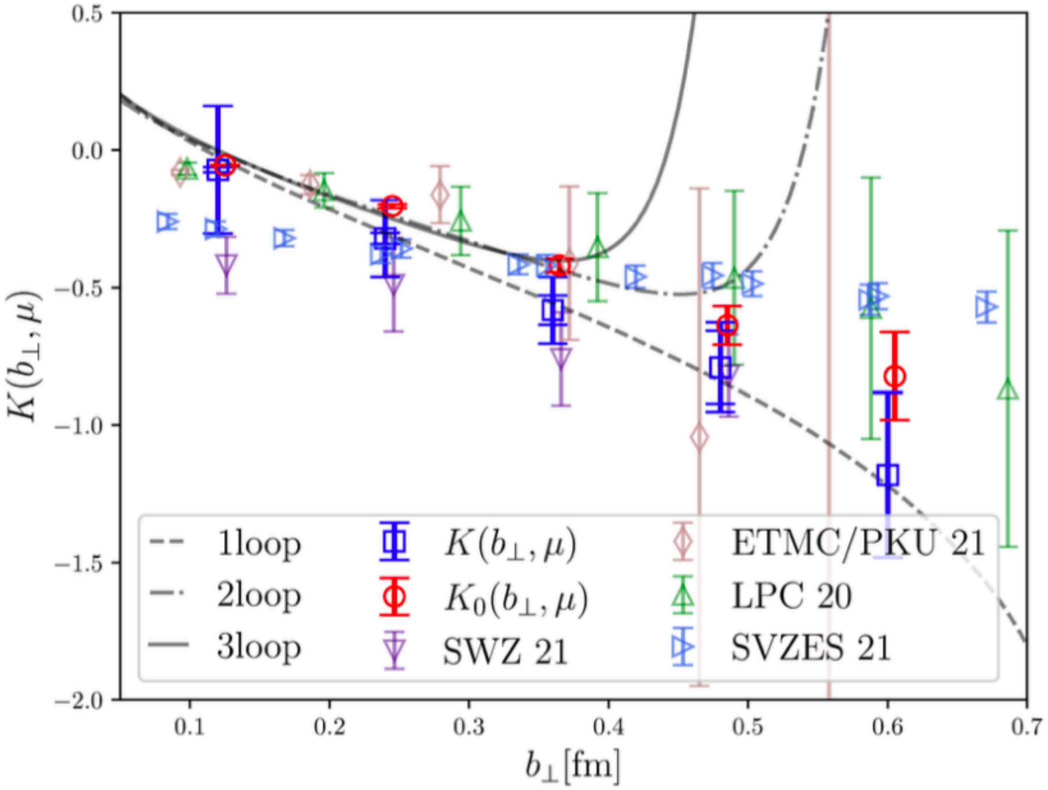

Systematics remain:

- One lattice spacing, no continuum limit
- Unphysical pion mass $m_\pi = 670\ \mathrm{MeV}$
- Operator mixing assumed to be negligible

Controlling LQCD systematics

Avkhadiev, Shanahan, MW, Zhao, PRD 108 (2023)

PRL 132 (2024)

- Larger boosts and (symmetric) staple extents using efficient TMD wavefunction codes reduce Fourier transform truncation effects

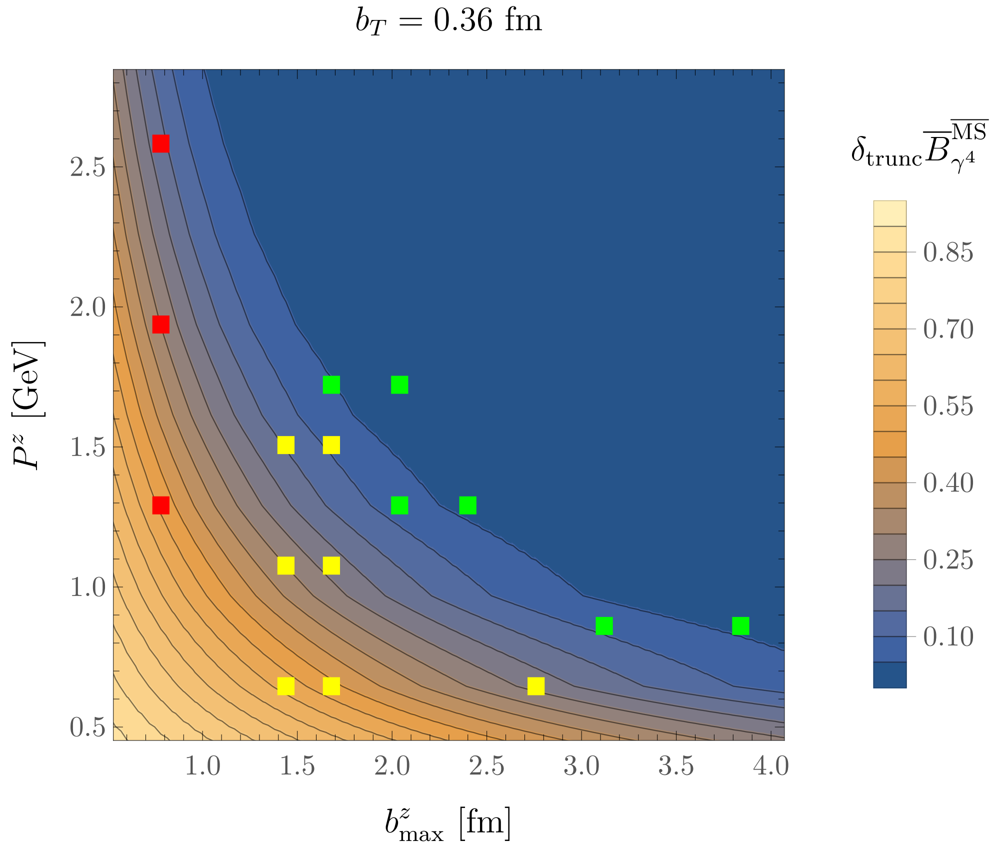

- Nearly physical quark masses

$$m_\pi = 149(1)\ \text{MeV}$$

- Continuum limit from 3 physical-mass ensembles with different lattice spacings

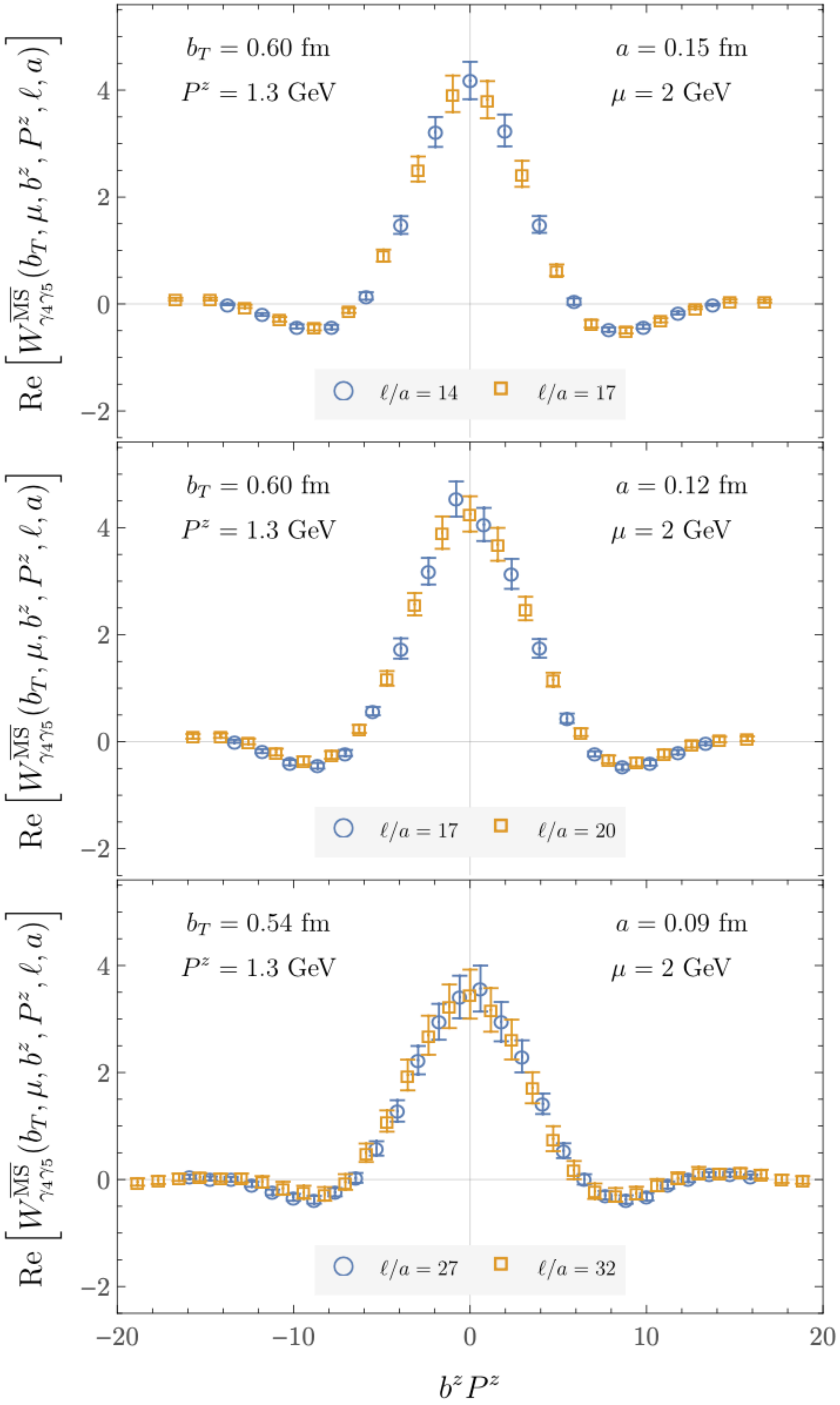

RI-xMOM renormalization

RI-xMOM renormalization scheme turns nonlocal operators into products of local operators by introducing auxiliary static quark fields

Ji, Zhang, and Zhao, PRL 120 (2018)

Green, Jansen, and Steffens, PRL 121 (2018)

Green, Jansen, and Steffens, PRD 101 (2020)

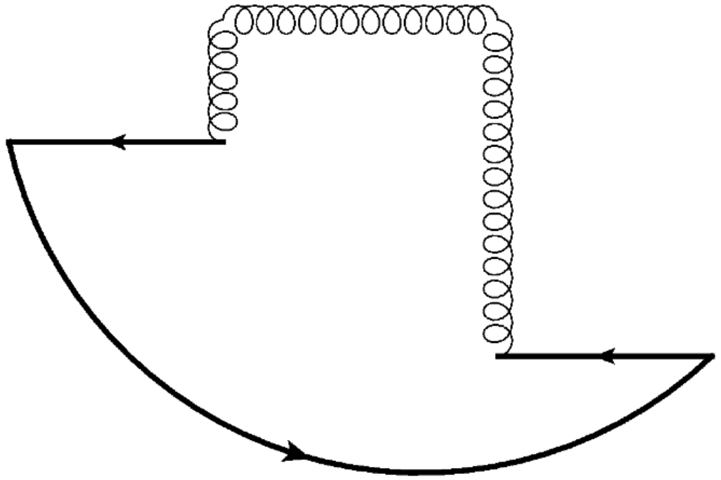

Operator mixing patterns agree with perturbative expectations

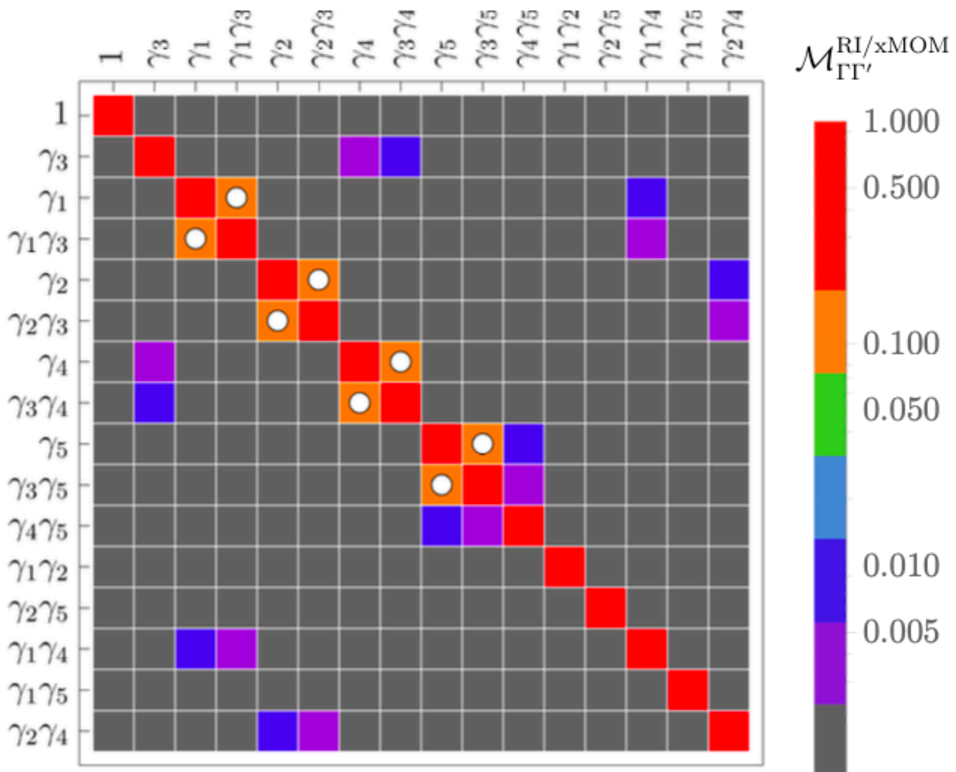

$a = 0.12$ fm, $p^\mu_{\mathrm{R}} = \frac{2\pi}{L} \times (0, 0, 10, 0)$, $\xi = 0.36$ fm

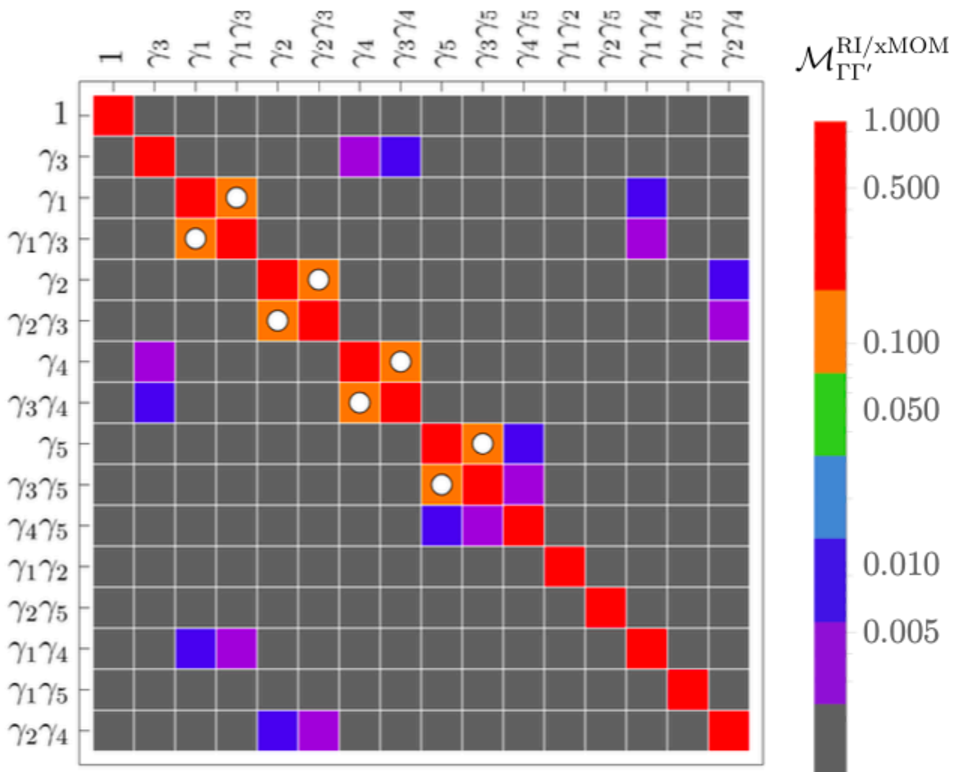

$a = 0.09$ fm, $p^\mu_{\mathrm{R}} = \frac{2\pi}{L} \times (0, 0, 10, 0)$, $\xi = 0.45$ fm

RI-xMOM renormalization

RI-xMOM renormalization scheme turns nonlocal operators into products of local operators by introducing auxiliary static quark fields

Ji, Zhang, and Zhao, PRL 120 (2018)

Green, Jansen, and Steffens, PRL 121 (2018)

Green, Jansen, and Steffens, PRD 101 (2020)

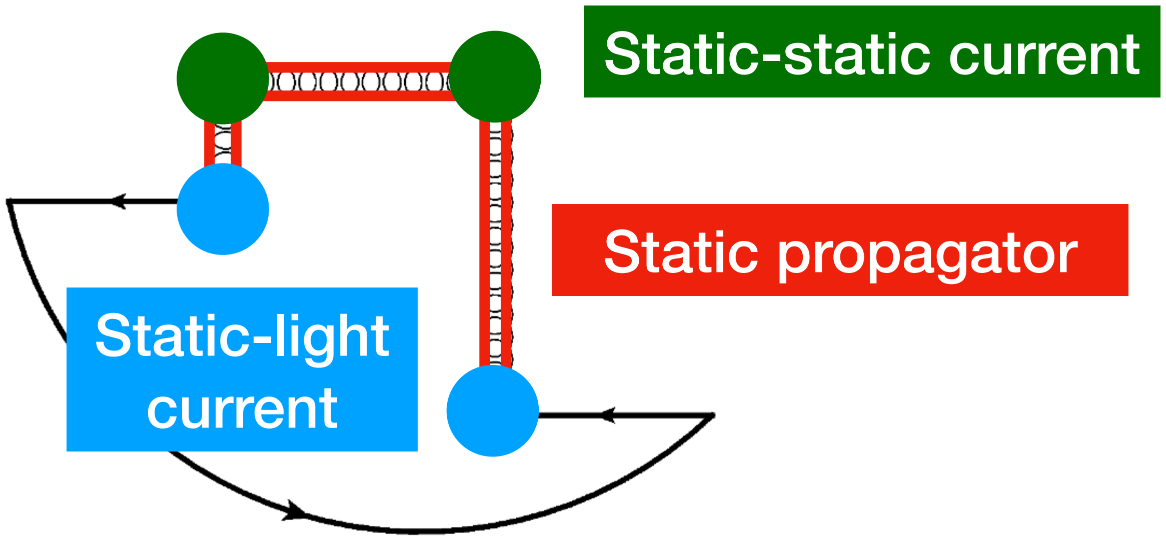

Operator mixing patterns agree with perturbative expectations

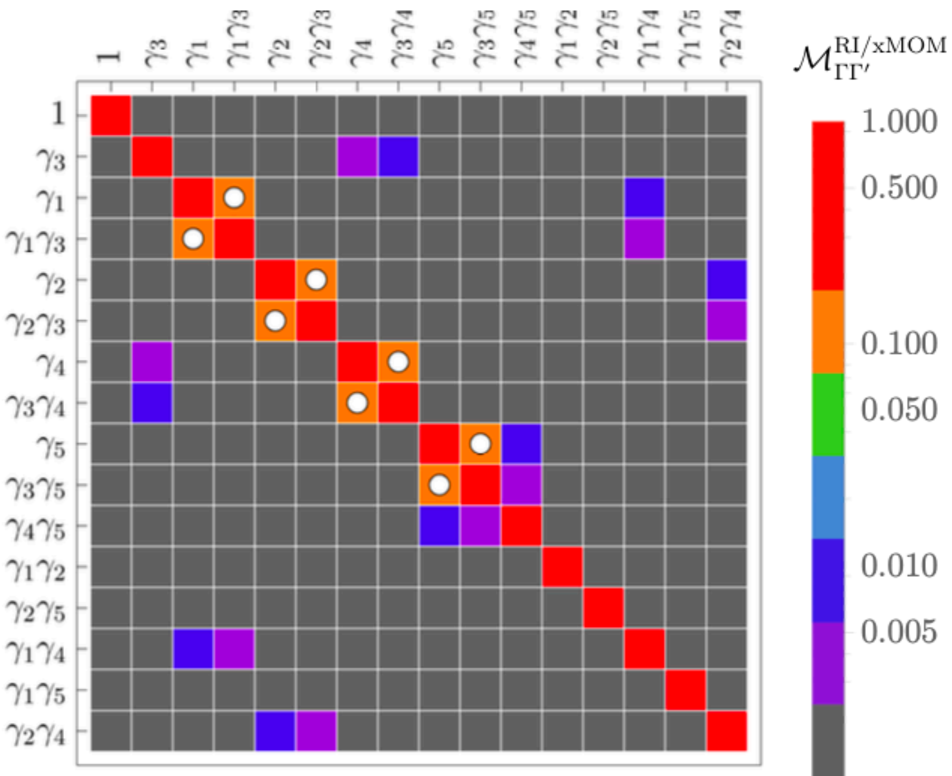

$a = 0.12$ fm, $p^\mu_{\mathrm{R}} = \frac{2\pi}{L} \times (0, 0, 10, 0)$, $\xi = 0.36$ fm

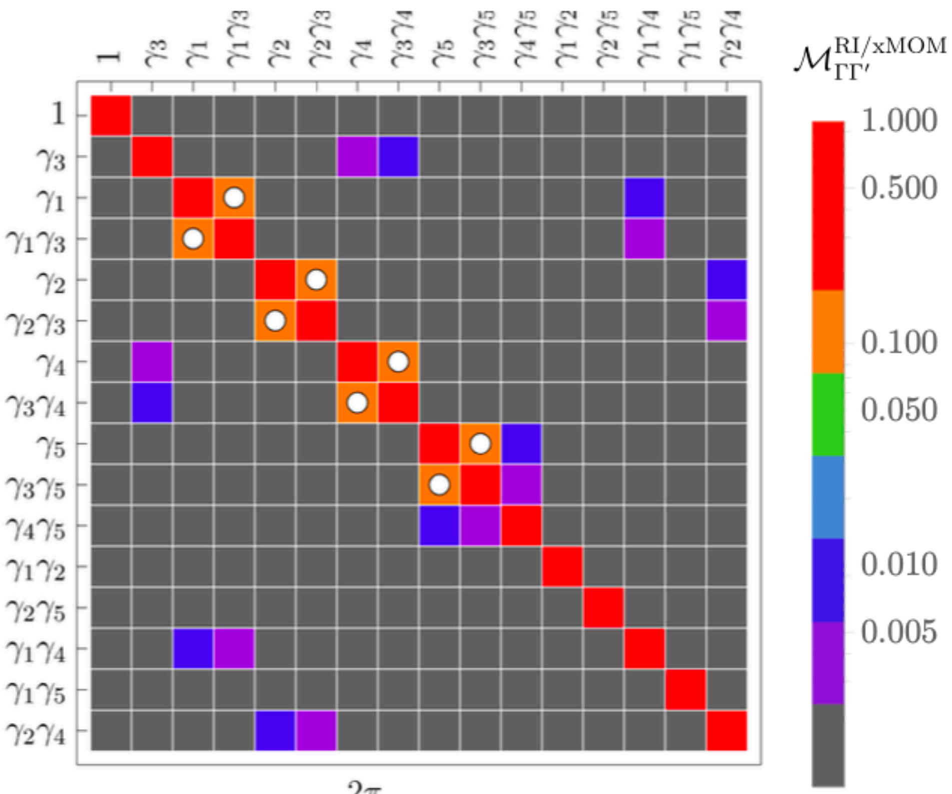

$a = 0.09$ fm, $p^\mu_{\mathrm{R}} = \frac{2\pi}{L} \times (0, 0, 10, 0)$, $\xi = 0.45$ fm

Discretization effects

New calculations used two additional MILC ensembles with nearly physical (valence and sea) pion masses

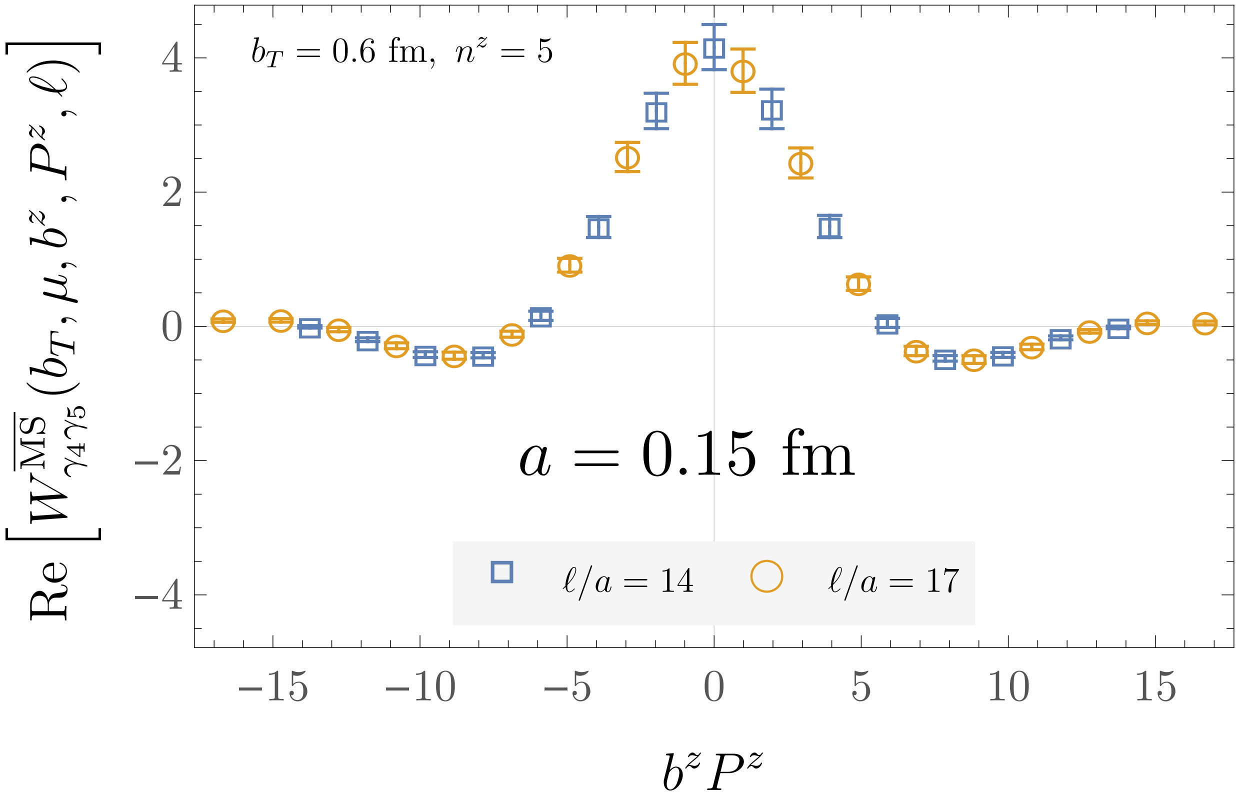

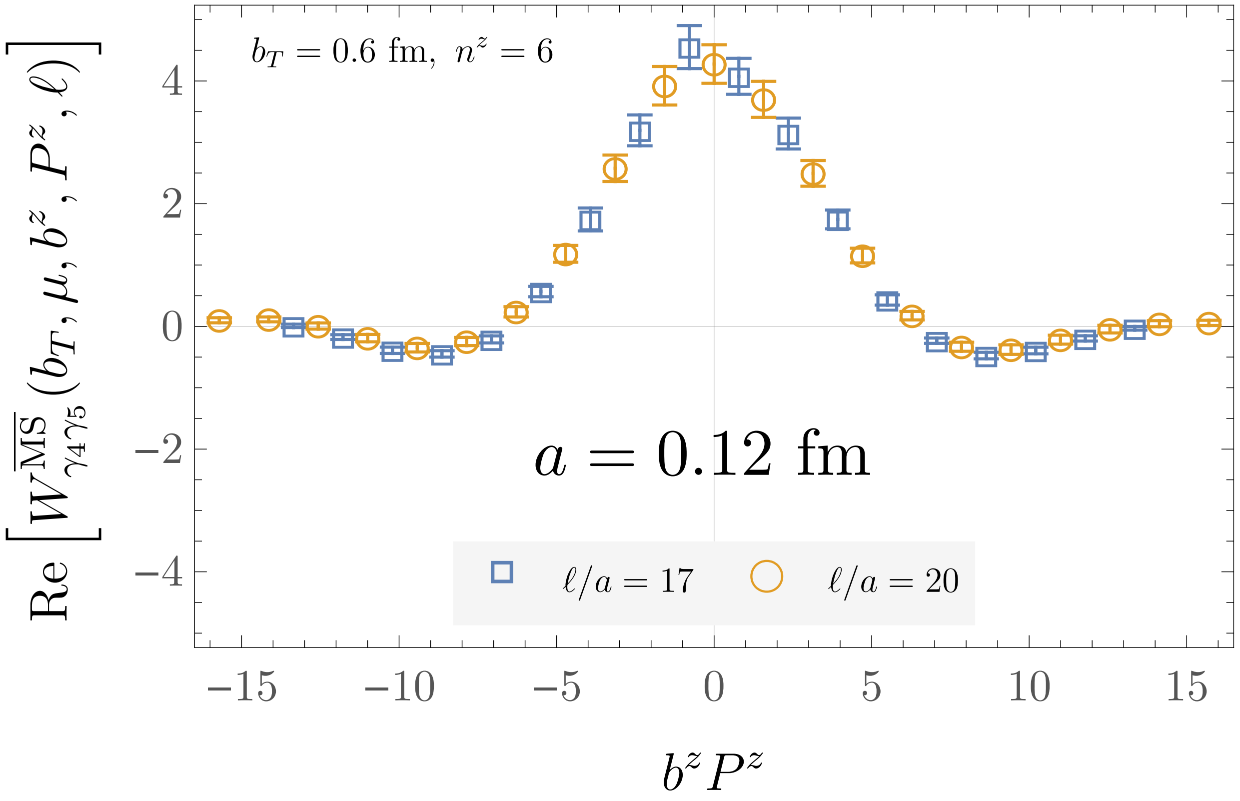

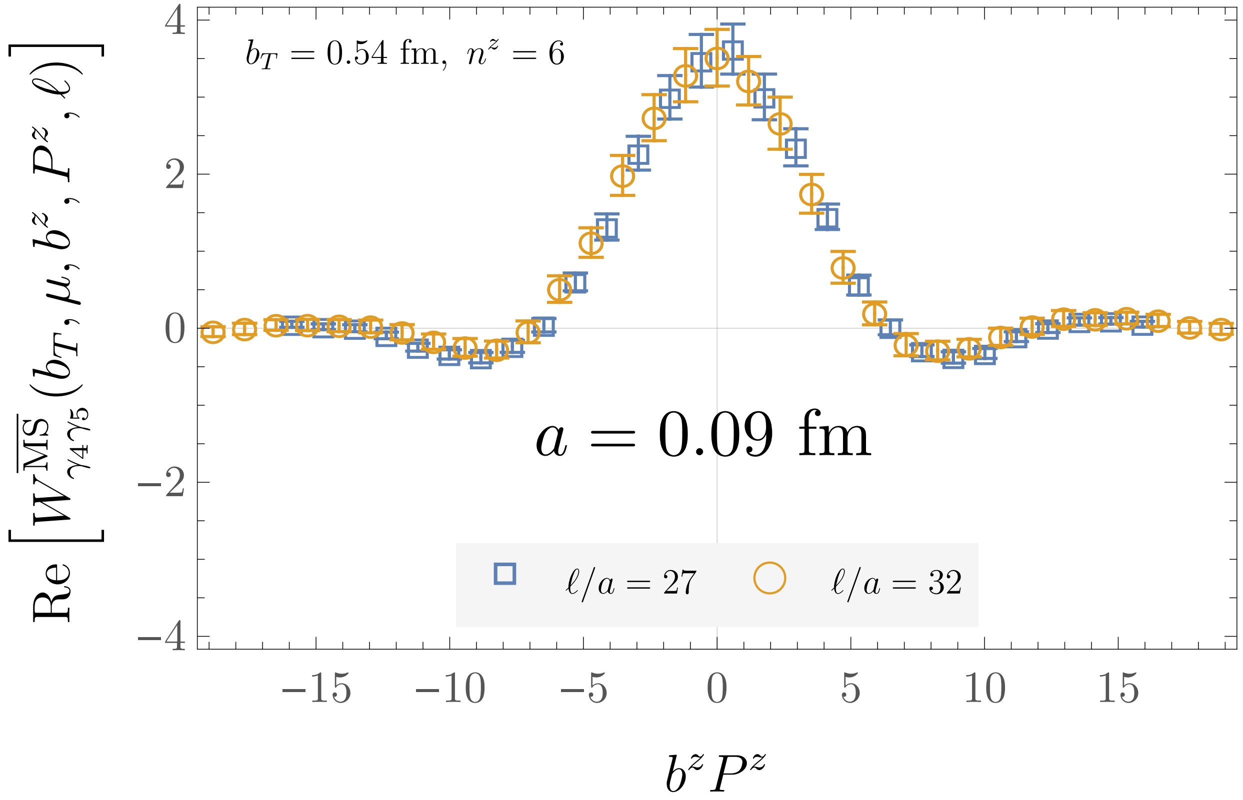

Avkhadiev, Shanahan, MW, Zhao, PRL 132 (2024)

Fourier transform ✓

Resulting renormalized TMD wavefunctions display expected symmetry in $b^z P^z$

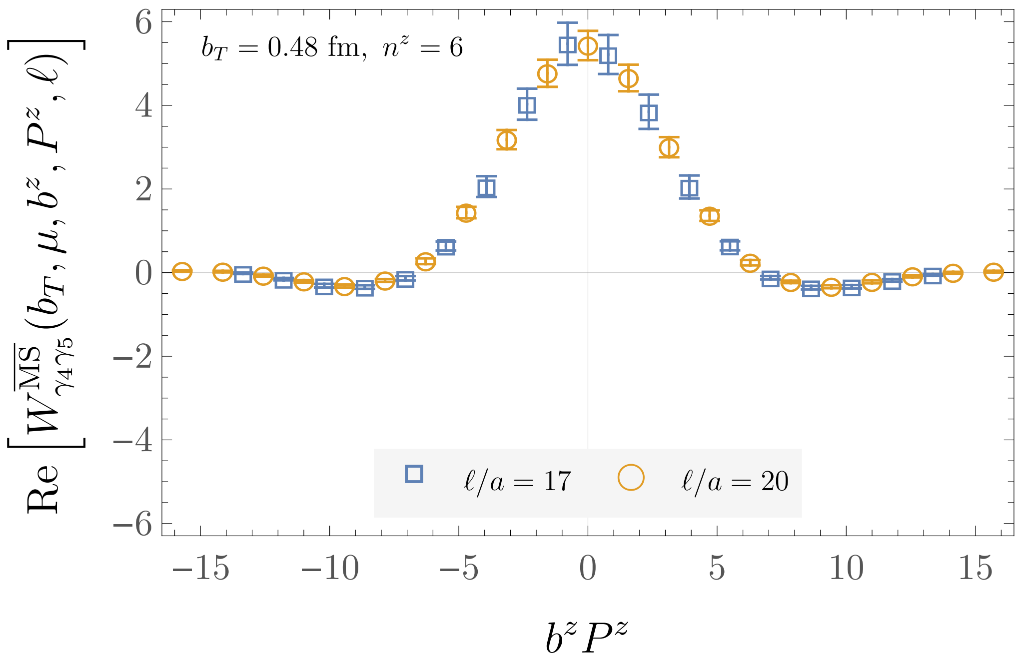

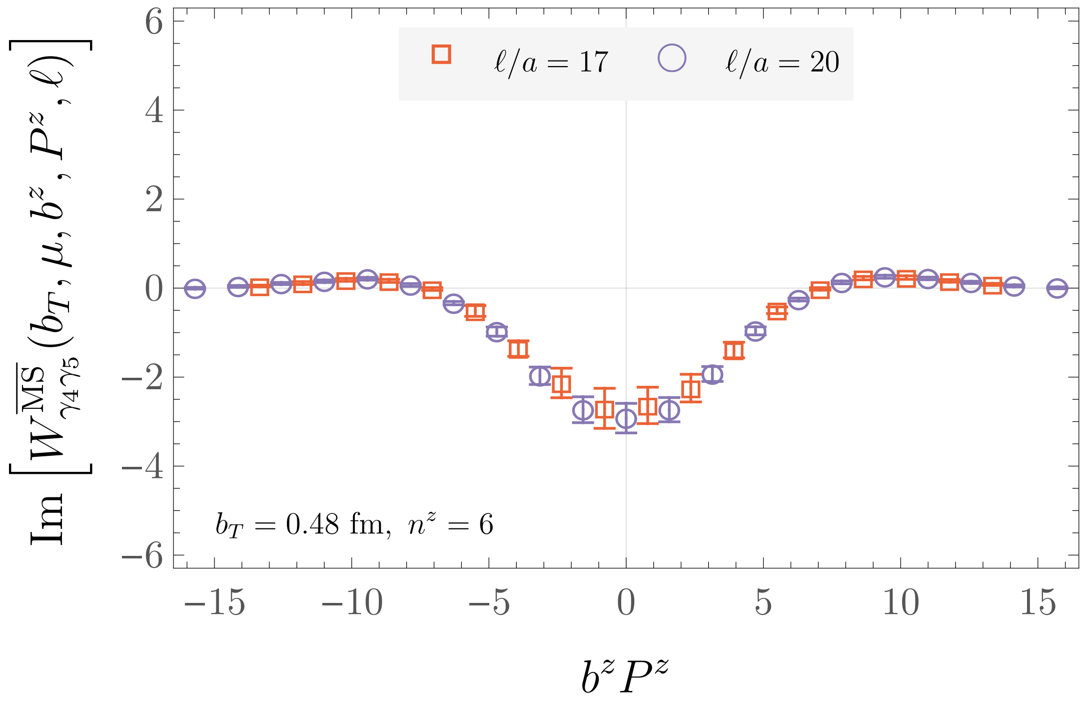

Large enough $b^z P^z$ achieved that simple DFTs show negligible truncation effects for all momenta studied

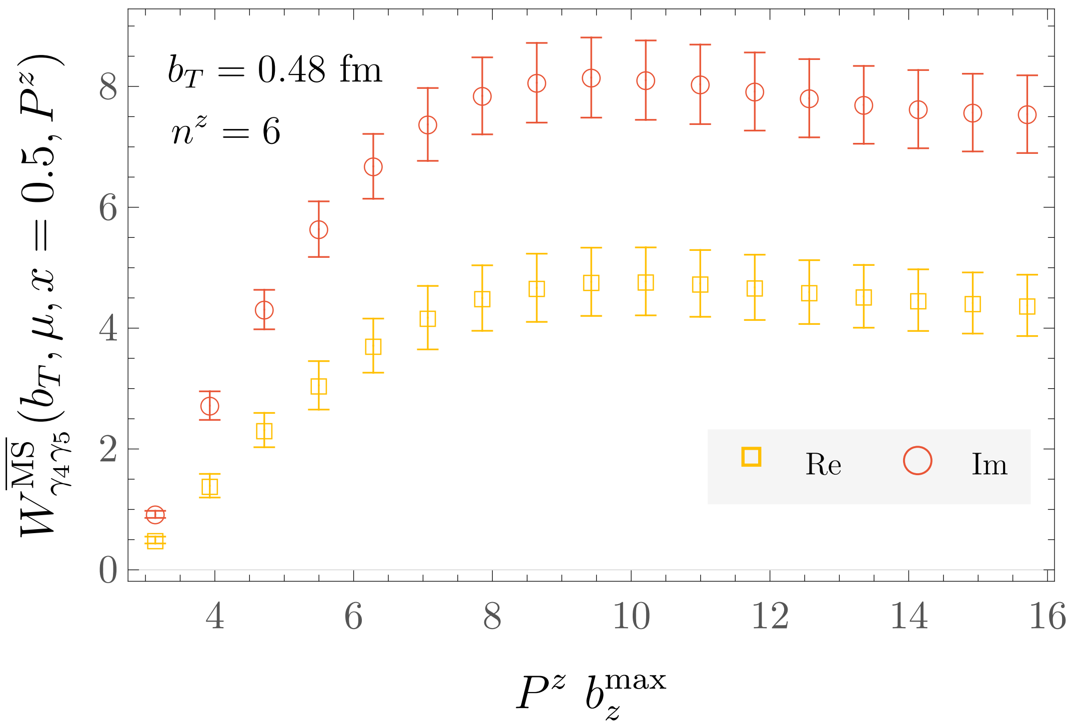

Avkhadiev, Shanahan, MW, Zhao, PRD 108 (2023)

Extracting the CS kernel

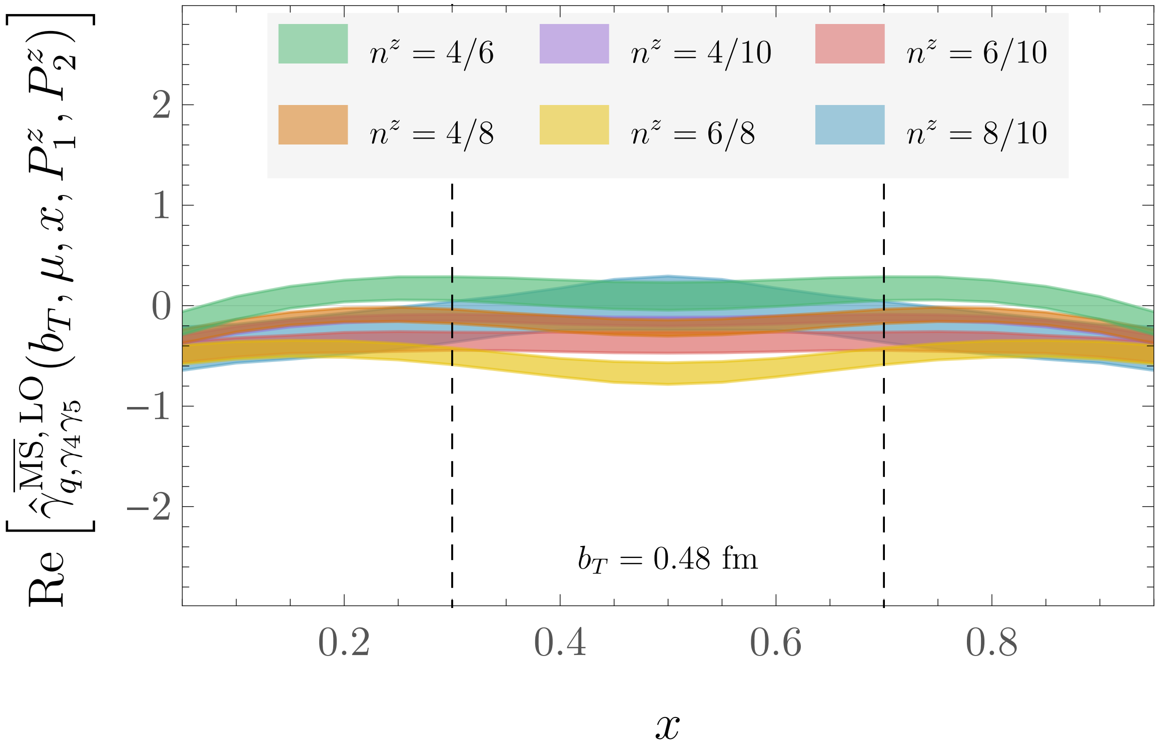

Ratios of TMD wavefunction DFTs show (asymptotically) expected x independence

CS kernel extracted from averaging over intermediate x and momentum pairs

LO, NLO, and NNLO perturbative matching shows clear convergence at large b_T

Resumed “unexpanded” matching improves small b_T convergence

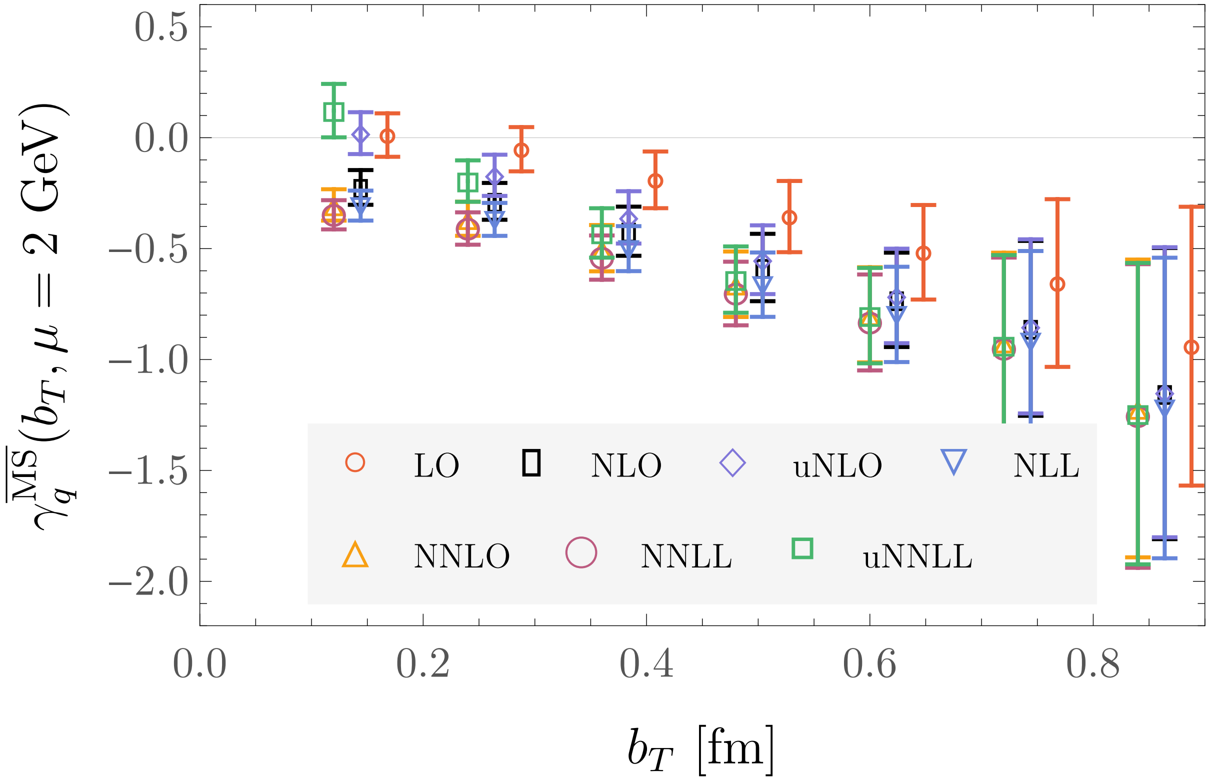

Avkhadiev, Shanahan, MW, Zhao, PRD 108 (2023)

Renormalon subtraction

Non-zero imaginary part of CS kernel unexpectedly appears after matching:

- Small b_T corrections to matching formula —- reduced by “unexpanded” resummed matching kernel. uNNLL matching affects Re and Im parts

  Avkhadiev, Shanahan, MW, Zhao, PRD 108 (2023)

- Renormalons — reduce with “leading-renomalon subtraction.” Only Im part

  Liu and Su, JHEP 2024 (2024)

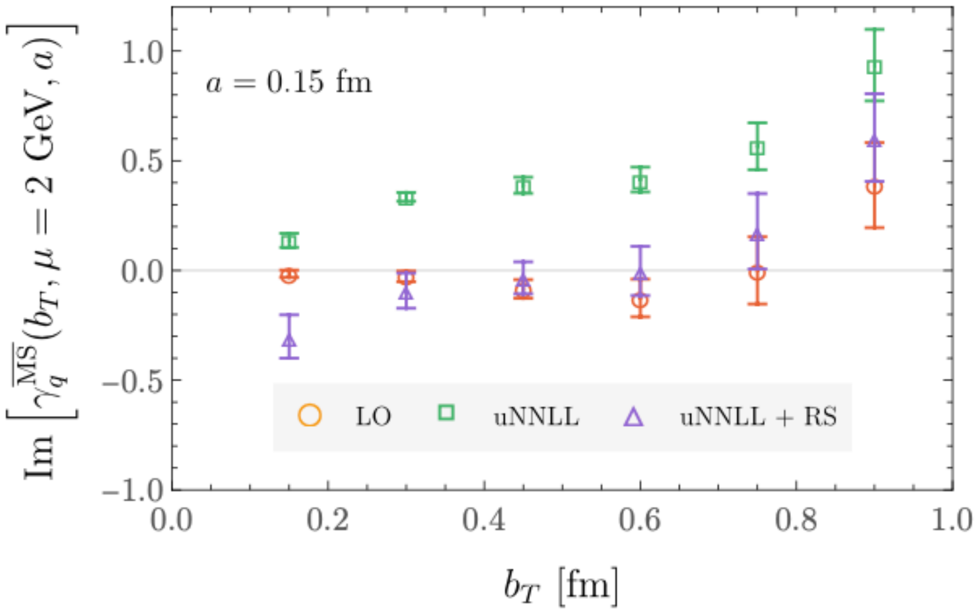

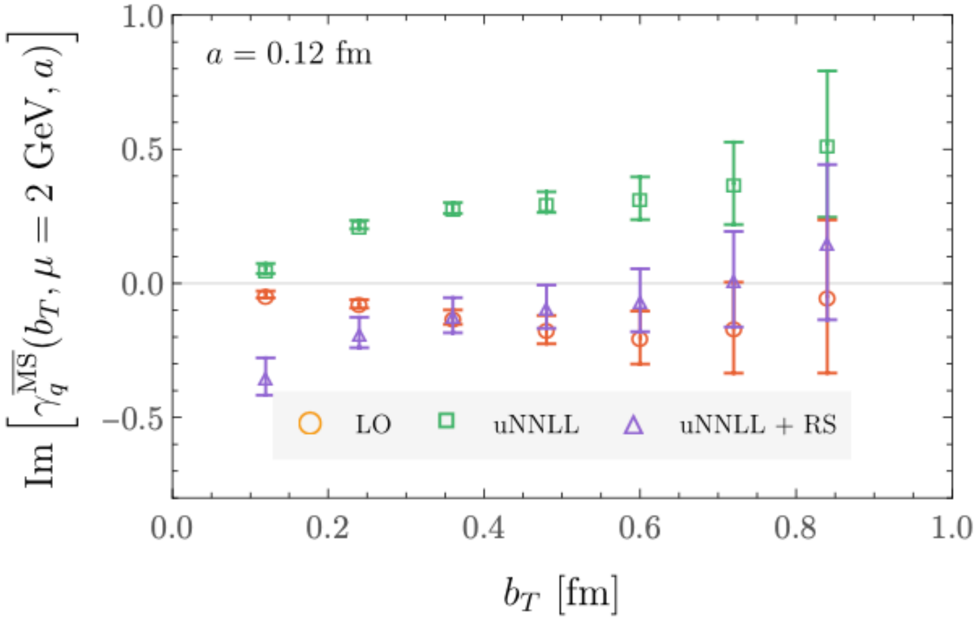

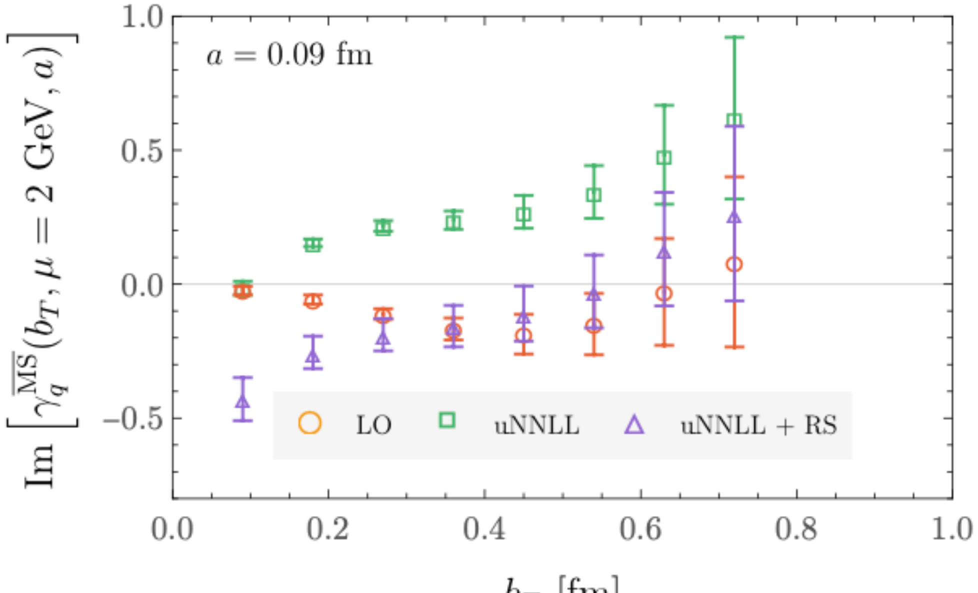

Avkhadiev, Shanahan, MW, Zhao, PRL 132 (2024)

The continuum limit

Discretization effects subtracted by fitting to parameterization of continuum CS kernel
+ lattice artifacts

$$\hat{\gamma}_q^{\overline{\mathrm{MS}}}(b_T, \mu, a) = \gamma_q^{\overline{\mathrm{MS}}}(b_T, \mu) + k_1 \frac{a}{b_T}$$

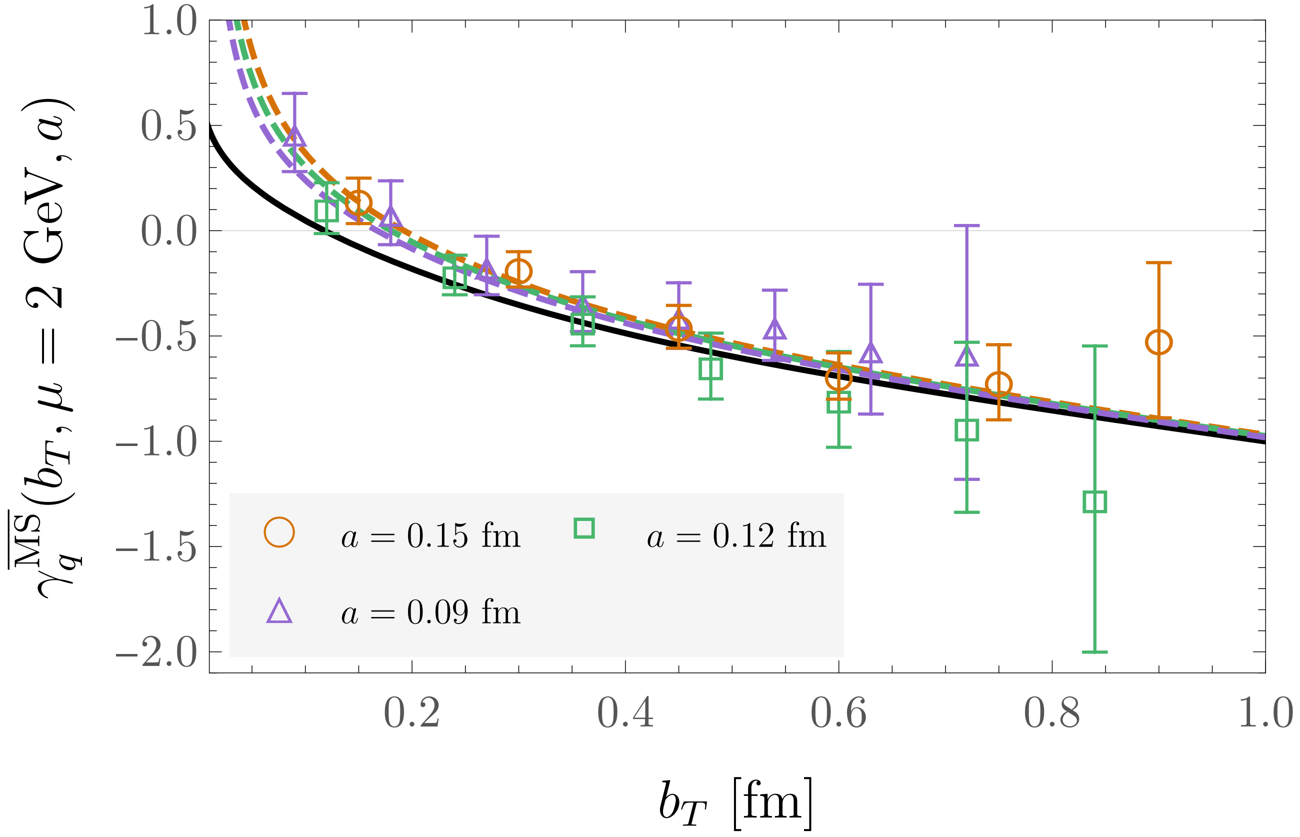

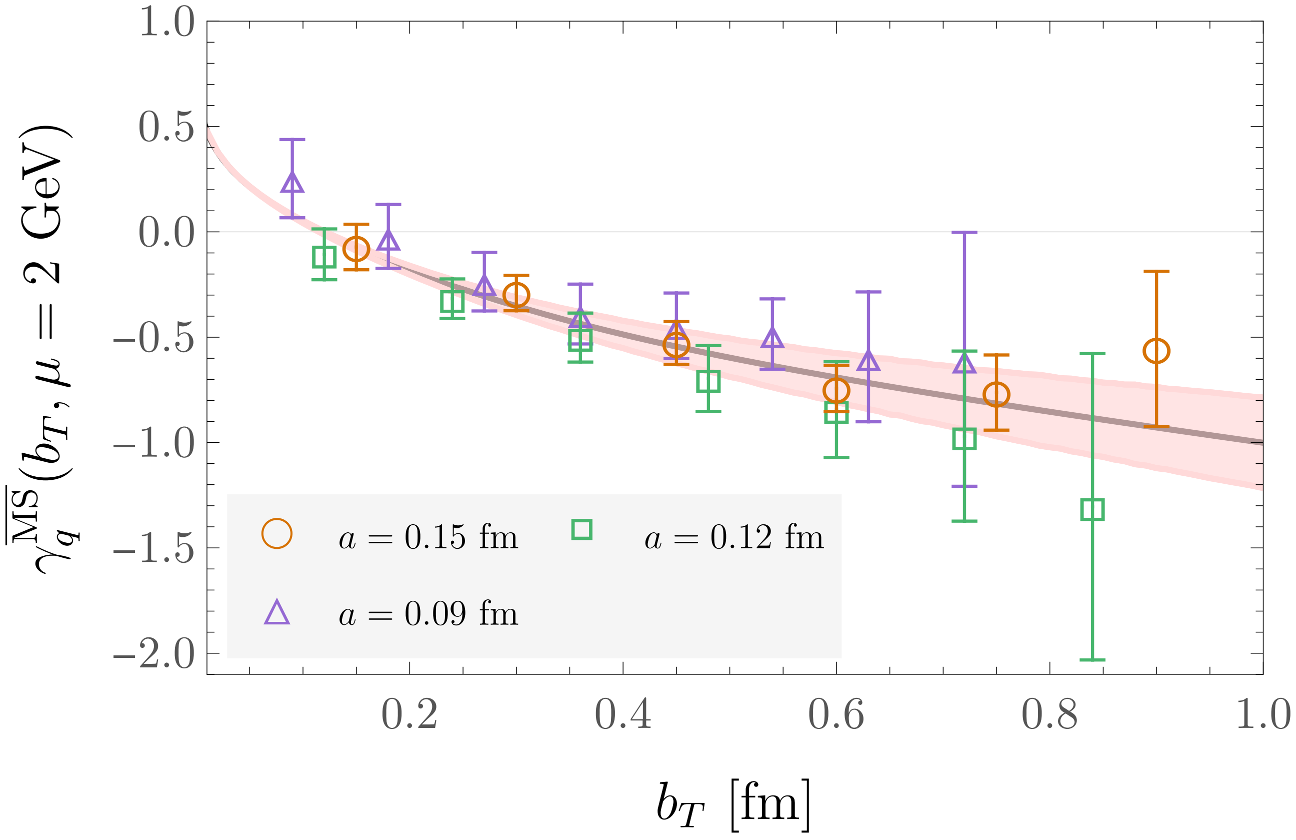

- Variety of other parameterizations, e.g. with $(a/b_T)^2$ terms, explored
- AIC used for data-driven model selection

Avkhadiev, Shanahan, MW, Zhao, PRL 132 (2024)

The CS kernel from LQCD

Continuum-limit LQCD results agree nicely with state-of-the-art phenomenological determinations of the CS kernel from global fits

LQCD precision is sufficient to exclude some models at large b_T

Avkhadiev, Shanahan, MW, Zhao, PRL 132 (2024)

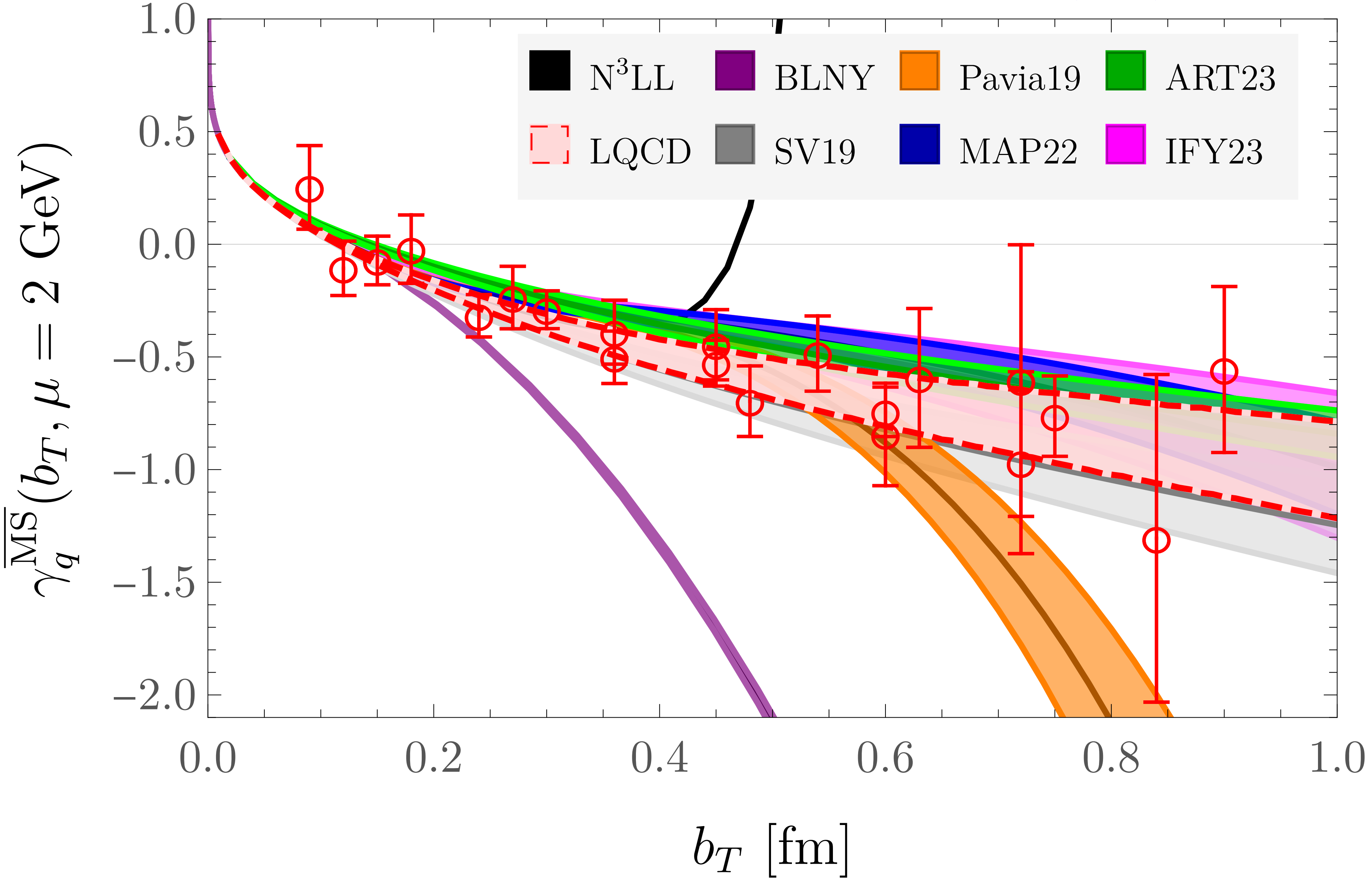

Continuum-limit LQCD results can be directly included in future global fits

LQCD CS kernel parameterization

Continuum-limit LQCD results can be directly included in future global fits by fixing CS kernel to pQCD+LQCD parameterization

$$\gamma_q^{\overline{\mathrm{MS}}}(b_T,\mu) = -2\mathcal{D}_{\mathrm{res}}(b^*(b_T),\mu) - 2\mathcal{D}_{\mathrm{NP}}(b_T)$$

$$b^*(b_T) = b_T/\sqrt{1 + b_T^2/(2\ \mathrm{GeV})^2}$$

$$\mathcal{D}_{\mathrm{res}}(b^*,\mu) = \int_{\mu_{b^*}}^{\mu} \frac{d\mu'}{\mu'}\Gamma_{\mathrm{cusp}}[\alpha_s(\mu')] + d[\alpha_s(\mu_{b^*})]$$

Avkhadiev, Shanahan, MW, Zhao, PRL 132 (2024)

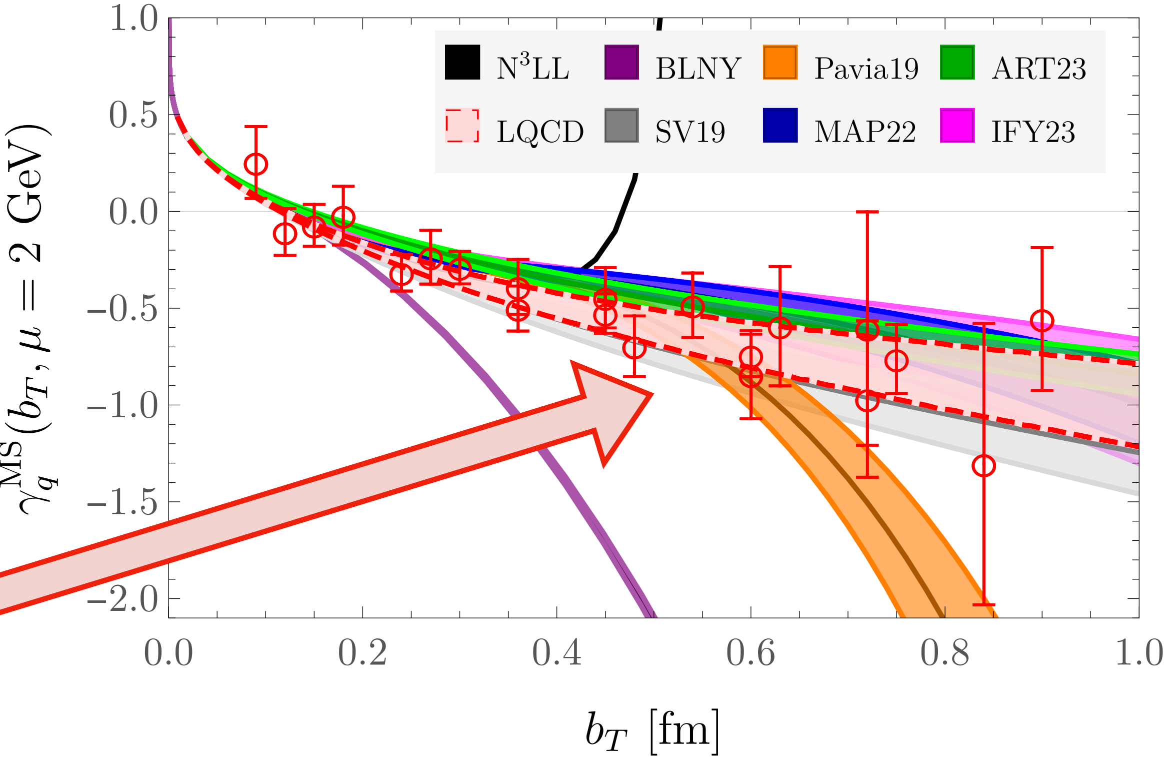

Nonperturbative effects can summarized by one parameter fit to LQCD data:

$$\mathcal{D}_{\mathrm{NP}}(b_T) = c_0 b_T b^*(b_T)$$

$$c_0 = 0.32(12)$$

$$\chi^2/\mathrm{dof} = 0.4$$

Other parameterizations with complementary physics interpretations possible, e.g. hadron structure oriented (HSO)

Aslan, Boglione, Gonzalez-Hernandez, Rainaldi, Rogers, and Simonelli, arXiv:2401.14266

$$b_K = 0.63(19)$$

$$\chi^2/\mathrm{dof} = 0.4$$

Towards TMDs from LQCD

Calculations of quasi-beam functions, quas-TMD wavefunctions, and the quasi-soft function can be combined to make complete predictions of TMDs

First exploratory LQCD calculations of nucleon TMDs performed by LPC Collaboration

Chu et al [LPC], PRD 109 (2024)

- One lattice spacing, three nucleon boosts, two quark masses

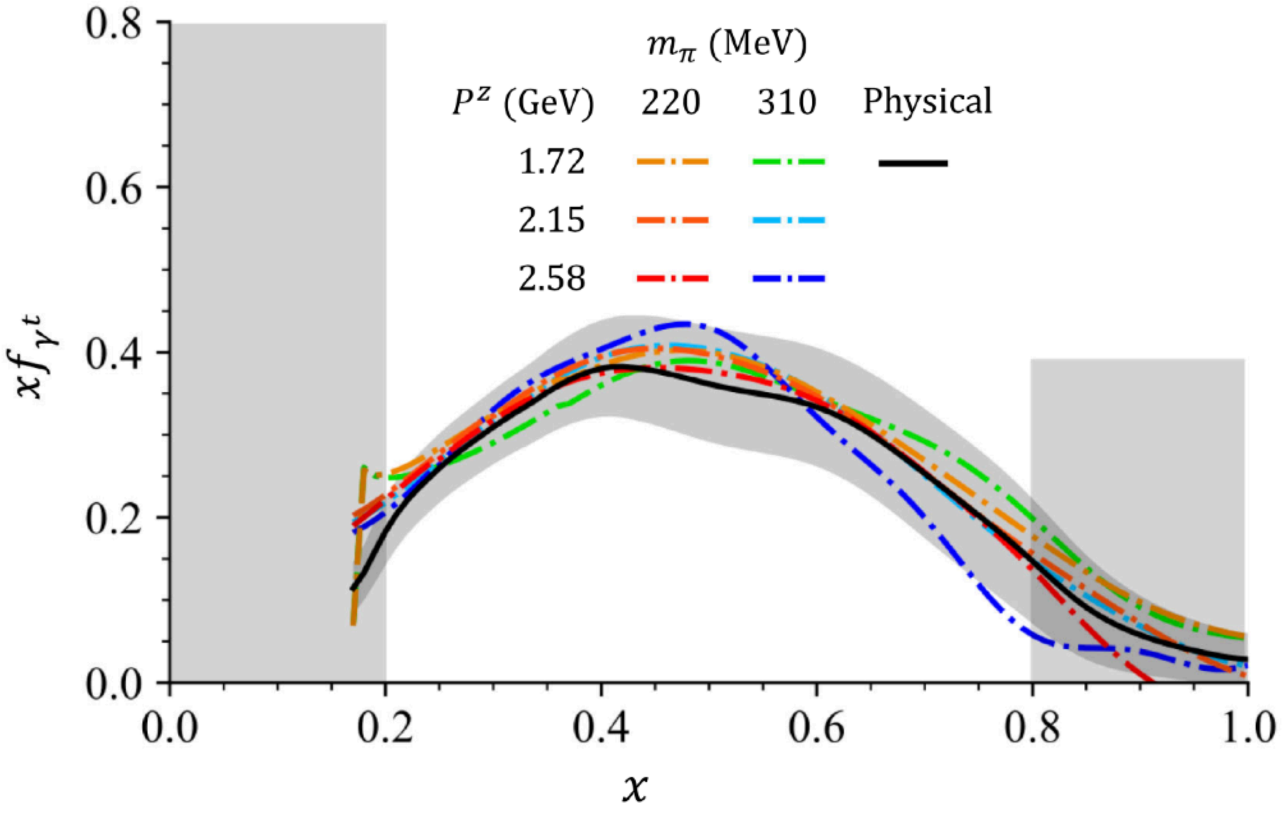

New techniques, e.g. Coulomb-gauge operator definitions, can further reduce computational cost

Gao, Liu, Zhao, PRD 109 (2024)

Zhao, arXiv:2311.10391

Exciting times ahead for TMD studies with LQCD

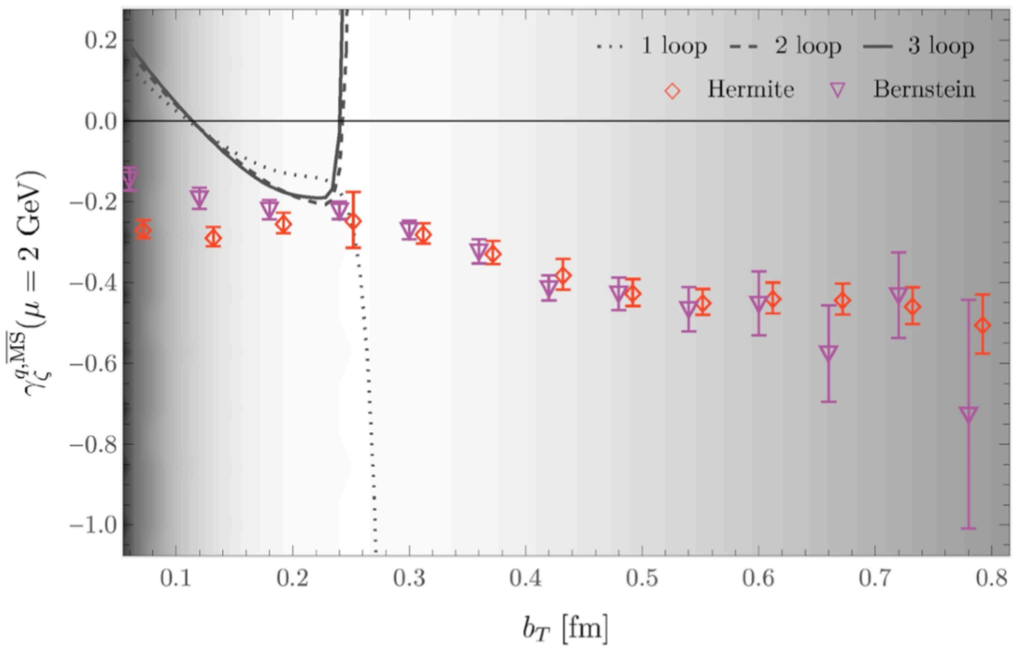
1 loop
2 loop
3 loop
Hermite
Bernstein
$\gamma_\zeta^{q,\overline{\mathrm{MS}}}(\mu = 2\ \mathrm{GeV})$
0.2
0.0
−0.2
−0.4
−0.6
−0.8
−1.0
0.1
0.2
0.3
0.4
0.5
0.6
0.7
0.8
b_T [fm]

Questions?

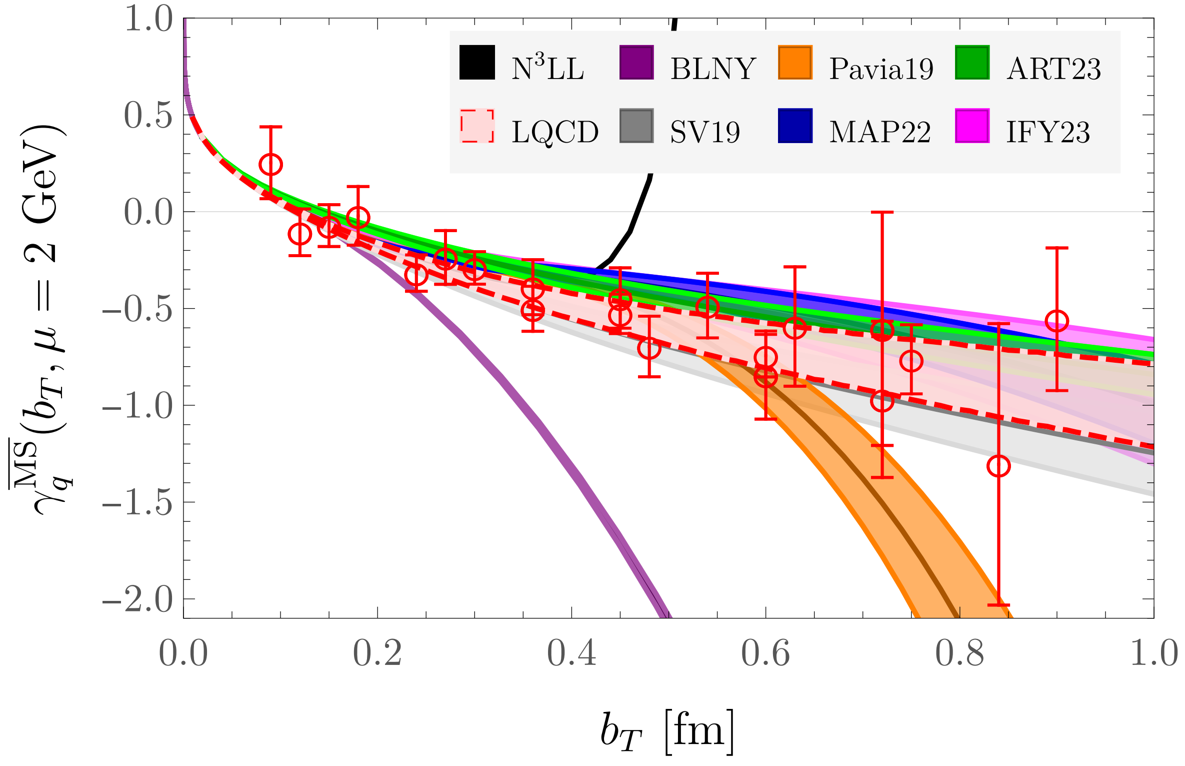
N^{3}LL
BLNY
Pavia19
ART23
LQCD
SV19
MAP22
IFY23
$\gamma_q^{\overline{\mathrm{MS}}}(b_T, \mu = 2\ \mathrm{GeV})$
1.0
0.5
0.0
−0.5
−1.0
−1.5
−2.0
0.0
0.2
0.4
0.6
0.8
1.0
b_T [fm]

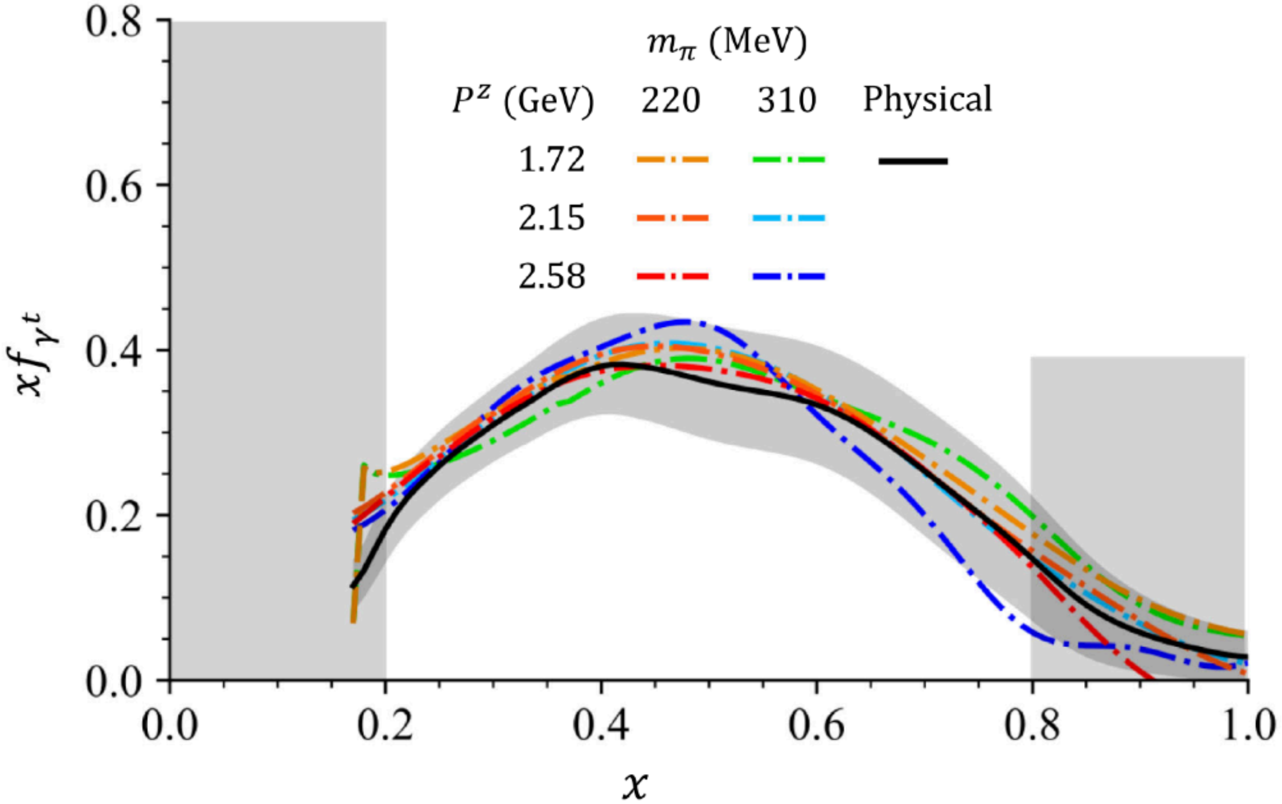
m_π (MeV)
P^z (GeV)
220
310
Physical
1.72
2.15
2.58
xf_{γ^t}
0.8
0.6
0.4
0.2
0.0
0.0
0.2
0.4
0.6
0.8
1.0
x

Backup

Lattice details

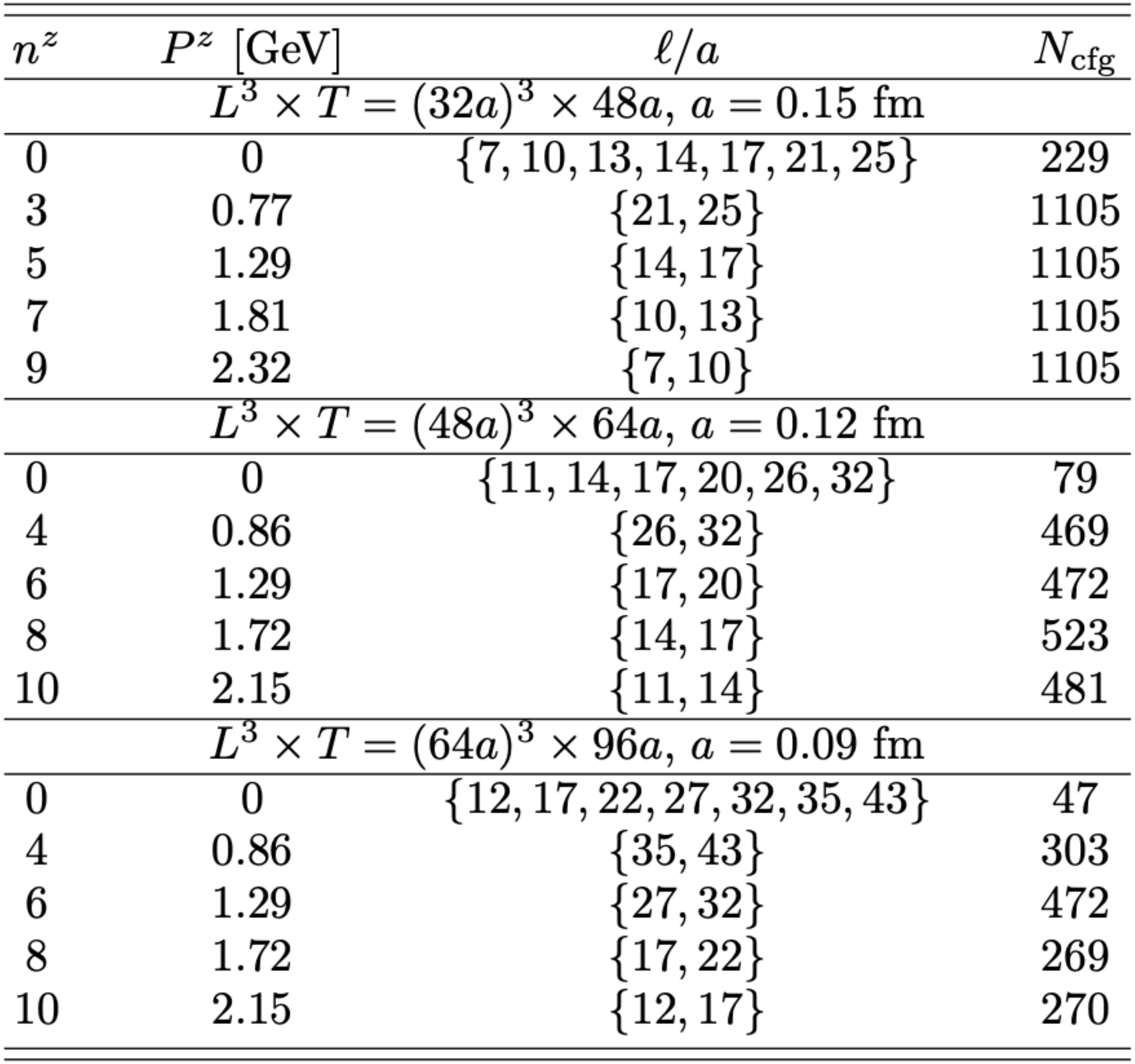

n^z	P^z [GeV]	ℓ/a	N_{cfg}
$L^3 \times T = (32a)^3 \times 48a,\ a = 0.15$ fm			
0	0	$\{7, 10, 13, 14, 17, 21, 25\}$	229
3	0.77	$\{21, 25\}$	1105
5	1.29	$\{14, 17\}$	1105
7	1.81	$\{10, 13\}$	1105
9	2.32	$\{7, 10\}$	1105
$L^3 \times T = (48a)^3 \times 64a,\ a = 0.12$ fm			
0	0	$\{11, 14, 17, 20, 26, 32\}$	79
4	0.86	$\{26, 32\}$	469
6	1.29	$\{17, 20\}$	472
8	1.72	$\{14, 17\}$	523
10	2.15	$\{11, 14\}$	481
$L^3 \times T = (64a)^3 \times 96a,\ a = 0.09$ fm			
0	0	$\{12, 17, 22, 27, 32, 35, 43\}$	47
4	0.86	$\{35, 43\}$	303
6	1.29	$\{27, 32\}$	472
8	1.72	$\{17, 22\}$	269
10	2.15	$\{12, 17\}$	270

Avkhadiev, Shanahan, MW, Zhao, PRL 132 (2024)

Fits

Too many fits to do each “by hand,” fully automated procedure for assigning fitting systematic uncertainty

- t_{min} — *results sensitive, take weighted average*

  Rinaldi, MW, et al, PRD 99 (2019)

  Jay and Neil, PRD 103 (2021)
- N_{states} — *results sensitive, take weighted average*
- t_{max} — *results insensitive (except when they’re not), impose arbitrary cut on signal-to-noise*
- *Covariance matrix — SVD, shrinkage, …*

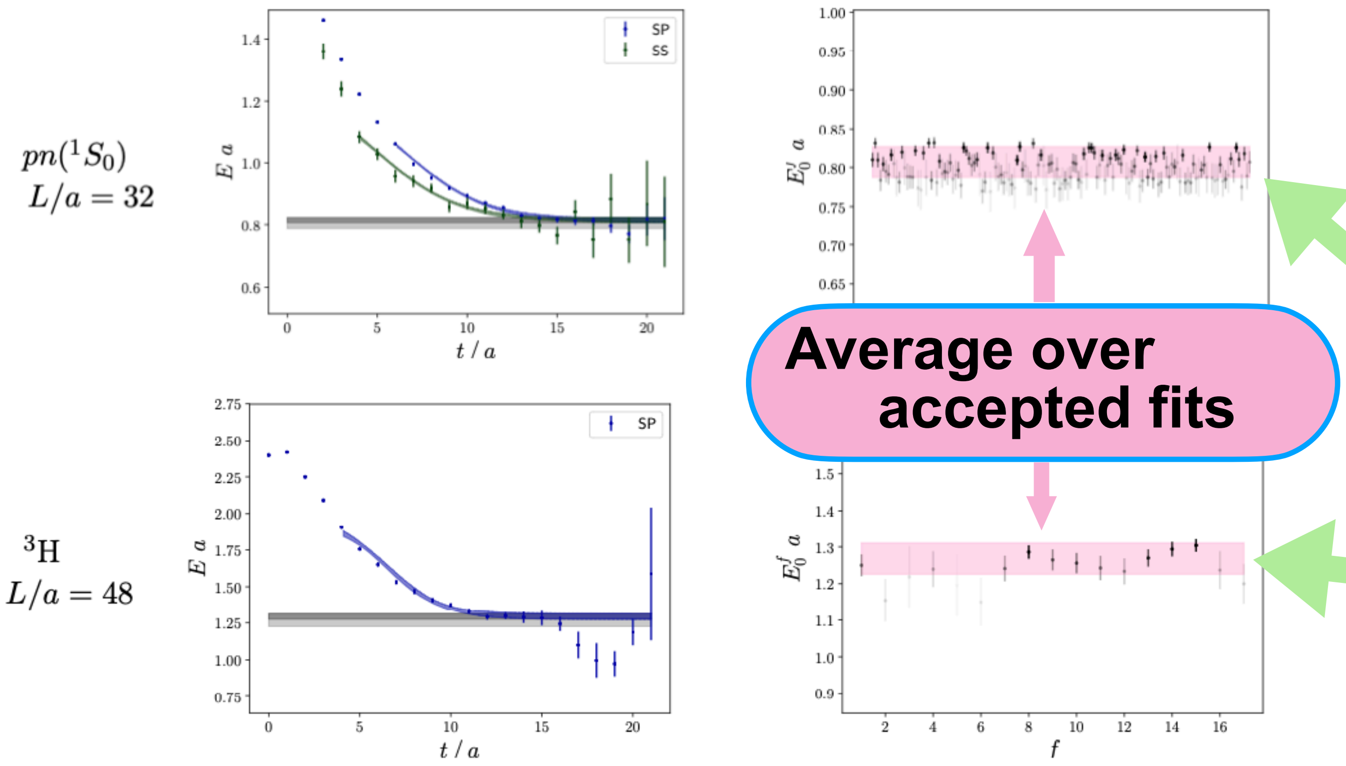

Average over accepted fits

“Autofitter” flowchart

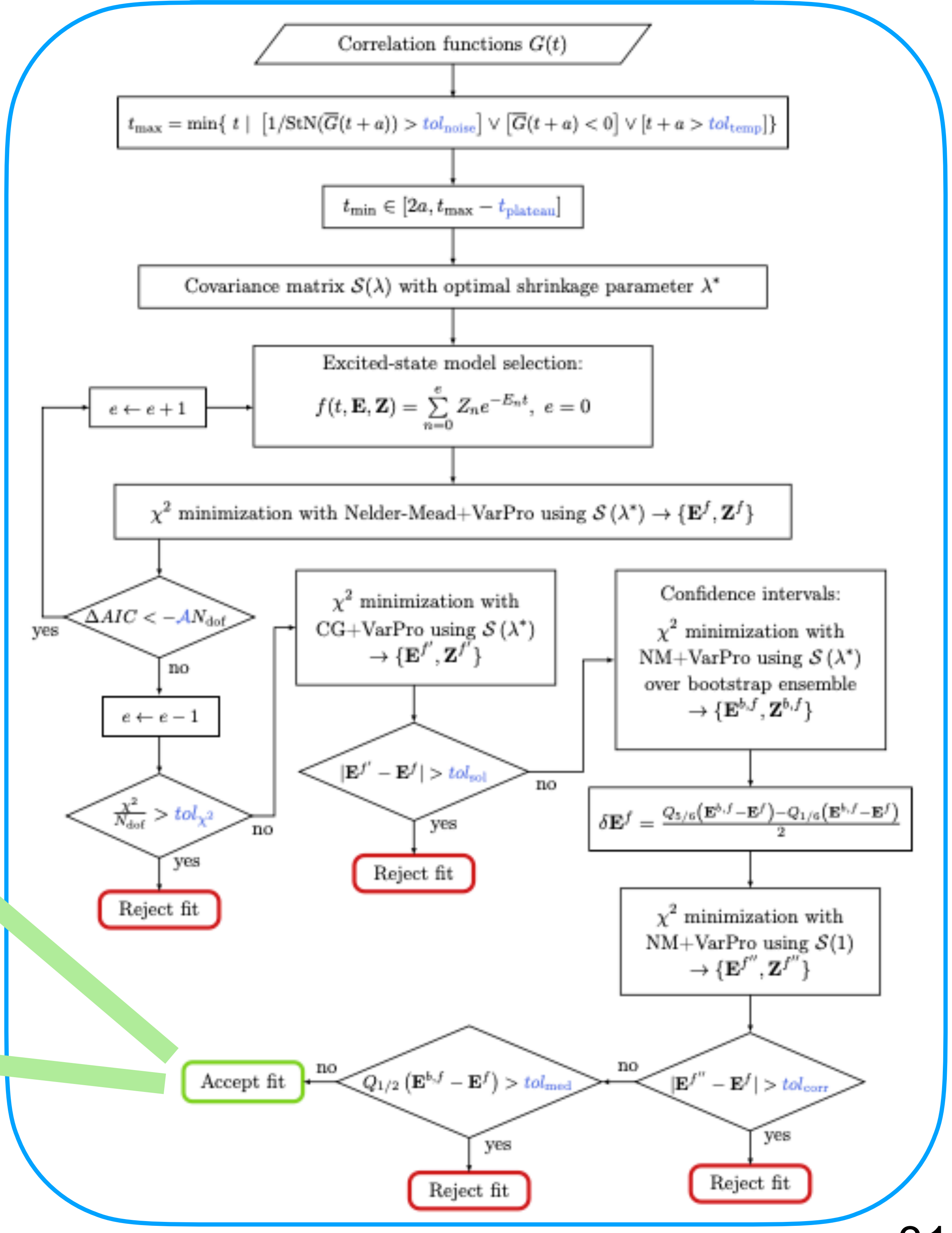

Beane, MW, et al [NPLCD+QCDSF+CSSM], PRD 103 (2021)